Section 2

SMART NANOTEXTILES FOR MEDICINE AND HEALTHCARE

2

Smart Nanotextiles for Wearable Health Monitoring

Shanshan Yao[1]*, Shuang Wu[2] and Yong Zhu[2]†

[1]Department of Mechanical Engineering, Stony Brook University, Stony Brook, NY, USA
[2]Department of Mechanical and Aerospace Engineering, North Carolina State University, Raleigh, NC, USA

Abstract

The rapid emergence of nanotechnology-enabled smart textiles provides new opportunities in health monitoring, therapeutic treatment, and disease management. Owing to the exceptional sensitivity, outstanding electric and mechanical properties, and scalable fabrication process, nanomaterials have become key building blocks for smart textiles. Wearable and personalized sensing greatly benefits tracking of health and wellness and treatment of illness through real-time and long-term monitoring of physiological indicators and physical activities. This chapter presents recent advances in nanotechnology-enabled smart textiles for health monitoring. The chapter starts with a brief overview followed by a summary of nanotextiles for sensing various physical biomarkers, including body temperature, biopotential signals, blood pulse, blood pressure, and respiration rate. Next, biochemical monitoring of key parameters in biofluids, breath, and body odor is highlighted. Finally, the development of sensors with multifunctionalities and the integration of multisensors for multimodal health monitoring are discussed.

***Keywords*:** Nanomaterial, nanostructure, nanotextile, health monitoring, wearable sensor

**Corresponding author*: shanshan.yao@stonybrook.edu
†*Corresponding author*: yong_zhu@ncsu.edu

Nazire Deniz Yilmaz (ed.) Smart Nanotextiles: Wearable and Technical Applications, (89–134) © 2022 Scrivener Publishing LLC

2.1 Introduction

Recent trends in personalized healthcare and telehealth have led to growing demands for real-time monitoring of physiological status and on-demand therapy [1–3]. Wearable health monitoring of key biomarkers and cues of diseases offers insights into the wellness of human body and the existence of health risks. The continuous monitoring in nonclinical settings provides new opportunities in point-of-care diagnostics and possible therapeutic interventions in the early stage [4–8].

Wearable health monitoring is achieved by seamlessly interfacing wearable sensors with the surface of human skin and tissues. Flexible and stretchable platforms based on both polymer and textile substrates are deployed to build up wearable devices [2, 9–11]. Textiles possess a series of merits including being soft, breathable, lightweight, flexible/stretchable, and comfortable to wear for an extended period of time. These features make them natural vehicles for constructing sensors that are in intimate contact with human body [12–14]. Nanomaterials, including 0D [e.g. nanoparticles (NPs)], 1D [e.g. nanowires (NWs), nanotubes (NTs), and nanofibers (NFs)], 2D [e.g. nanowebs, graphene, graphene oxide (GO), reduced graphene oxide (rGO), molybdenum disulfide (MoS_2), and MXenes], have been incorporated as building blocks for smart nanotextiles, owing to their large surface-to-volume ratio, exceptional material properties, and compatibility with scalable fabrication methods (e.g., printing) [6, 15]. The synergic combination of nanomaterials and textiles renders desirable flexibility and stretchability to accommodate repeated skin deformations during daily activities, allowing for precise and unobtrusive health monitoring with minimal user discomfort.

Nanomaterials can be incorporated into fibrous assemblies at different levels, by the introduction of nanomaterials during the fabrication of fibers/yarns or by surface modifications at the fabric or textile level [13, 14]. Several manufacturing techniques have been applied to construct nanotextiles that achieve seamless hybridization between nanomaterials and textiles, including sewing, knitting, weaving, embroidering, spinning, drawing, coating, and printing [10, 13, 16, 17]. Deformable structures, such as twisted, helical, buckling, and winding structures, can also be introduced to impart high stretchability beyond the intrinsic properties of textiles [12]. These nanotextiles can be formed into various wearable form factors, such as belts, bandages, patches, contact lenses, gloves, socks, and sportswear (Tables 2.1–2.3).

Table 2.1 Summary of nanotextiles for (bio)physical monitoring.

Refs	Sensing locations	Sensing platforms	Biomarkers	Applications
[31]	Hand	Skin patch	Temperature	Wireless temperature sensing and on-demand anti-infection therapy at wound sites
[25]	Mouth/hand/nose	Fiber	Temperature	Monitoring of temperature and thermal activities of mouth, hand, and nose breathing
[32]	Palm	Skin patch	Temperature	Spatial temperature mapping
[30]	In front of mouth/nose	Fiber patch	Temperature	Monitoring of temperature in mouth respiration and nose breathing
[33]	Scapula/armpit/upper chest/upper arm/paravertebral/lower arm/abdomen	Fabric sensing network	Temperature	*In situ* detection of skin temperature during respiration
[28]	–	Fiber	Temperature	Supercapacitor driven temperature sensing
[27]	–	Fiber	Temperature	Temperature sensing, electrocapillary sucker

(*Continued*)

Table 2.1 Summary of nanotextiles for (bio)physical monitoring. (*Continued*)

Refs	Sensing locations	Sensing platforms	Biomarkers	Applications
[45]	Left/right finger	Cotton patch	ECG	Heart rate monitoring
[44]	Left/right wrist	Nylon fiber patch	ECG	ECG recording
[43]	Left/right arm	Woven cotton patch	ECG	ECG recording
[42]	Left/right arm	Cotton patch	ECG	ECG recording
[51]	Thorax	Nanofiber web	ECG	ECG recording
[50]	Eye	Contact lens	ERG	Full-field ERG recordings
[41]	Left/right arm/ left leg/distal phalanges/ head/earlobe	Nonwoven fabric	EMG/ECG/ EEG/EDA	Wireless biopotential measurements, strain sensing, superhydrophobic sheet, heat-dissipation sheet, electrothermal heater
[60]	Wrist	Silk wrist band	Blood pulse	Arterial pulse monitoring, external pressure sensing
[68]	Wrist/neck	Nanofiber mat	Blood pulse	Radial and carotid pulse monitoring
[69]	Wrist	Nanofiber mat	Blood pulse	Wrist pulse monitoring
[67]	Wrist	Skin patch	Blood pulse	Wrist pulse monitoring, external pressure/ shear/torsion sensing

(*Continued*)

Table 2.1 Summary of nanotextiles for (bio)physical monitoring. (*Continued*)

Refs	Sensing locations	Sensing platforms	Biomarkers	Applications
[74]	Artificial blood vessel	Nanofiber sheet	Blood pressure	Monitoring of the pressure propagation from the artificial blood vessel
[75]	Wrist	Wrist band	Blood pressure	Blood pressure monitoring, external pressure mapping
[91]	Mouth	Face mask	Respiration	Respiration monitoring during normal/deep/fast breathing

Table 2.2 Summary of nanotextiles for (bio)chemical monitoring.

Refs	Sensing locations	Sensing platforms	Biomarkers	Applications
[102]	Whole body	Garment	Glucose/ $Na^+/K^+/Ca^{2+}$/pH in sweat	Real-time wireless analysis of the sweat during running
[103]	Waist/wrist/leg	Underwear/watch strap/elastic band	Na^+/K^+ in sweat	Wireless analysis of multi-ions in sweat
[105]	Foot ankle	Socks	Glucose/lactate in sweat	Real-time wirelessly sensing of lactate during cycling

(*Continued*)

Table 2.2 Summary of nanotextiles for (bio)chemical monitoring. (*Continued*)

Refs	Sensing locations	Sensing platforms	Biomarkers	Applications
[100]	Upper back	Textile patch	Na^+ in sweat	Real-time monitoring of sodium concentration in sweat during cycling
[101]	Right deltoid	Skin-worn tattoo	Lactate in sweat	Real-time monitoring of sweat lactate dynamics during cycling
[98]	Wrist	Silk film	Glucose in sweat	Monitoring of sweat glucose on the wrist
[108]	Eye	Contact lens	Glucose in tear	Wirelessly monitoring and visualization of glucose concentration in tear
[115]	Urine/ armpit/ exhaled breath	Cotton satin patch	VOCs in urine/ armpit/ exhaled breath	Wearable electronic nose for monitoring and discriminating human body odor
[111]	In front of nose/ breath	Optical fiber	Humidity in exhaled breath	Monitoring of breath frequency and depth
[113]	In front of mouth	Fiber	Humidity in exhaled breath	Real-time wireless detection of breath humidity
[112]	In front of nose/ mouth	Textile patch	Humidity in mouth/ nose breath	Monitoring of humidity in mouth/nose breath and sweating, electromagnetic interference shielding, self-derived hydrophobicity

Table 2.3 Summary of nanotextiles for multimodal physiological monitoring.

Refs	Sensing locations	Sensing platforms	Biomarkers	Applications
[130]	Wrist	Skin patch	Wrist temperature/ pulse	Monitoring of wrist temperature/ pulse, detection of external NIR illumination/ temperature/ pressure
[131]	Neck/ shoulder/ chest/ waist/ wrist/ finger	Smart sportswear	Body temperature/ blood pulse/ respiration/ phonation/ muscle movement/ body motion	Monitoring of body temperature/ pulse/ respiration/ swallowing/ phonation/ stretching exercise/ walking/chest expanding/ finger bending/ side twist, self-cooling
[125]	Wrist/throat	Silk fabric patch	Blood pulse/ phonation	Monitoring of pulse/ phonation, lithium-ion batteries
[141]	Wrist/finger/ under foot	Skin patch	Blood pulse/ body motion	Monitoring of wrist pulse/ finger bending/ walking/ running

(*Continued*)

Table 2.3 Summary of nanotextiles for multimodal physiological monitoring. (*Continued*)

Refs	Sensing locations	Sensing platforms	Biomarkers	Applications
[142]	Wrist/ forearm	Skin patch	Blood pulse/ body motion	Monitoring of wrist pulse/ finger flexion and extension, detection of external tactile distribution
[61]	Wrist/finger	Skin patch	Blood pulse/ body motion	Monitoring of wrist pulse/ finger bending, detection of external pressure distribution
[143]	Wrist/eye/ finger	Bandage/ strip	Blood pulse/ eyeball movement/ body motion	Monitoring of wrist pulse/ eye rotation, blinking, and movement during sleep/ finger bending, detection of external tactile distribution
[126]	Wrist/ throat/ finger	Fiber patch	Blood pulse/ phonation/ body motion	Monitoring of wrist pulse/ phonation/ finger bending
[66]	Wrist/ throat/ cheek	Skin patch	Blood pulse/ phonation/ muscle movement	Monitoring of wrist pulse/ phonation/ chewing

(*Continued*)

Table 2.3 Summary of nanotextiles for multimodal physiological monitoring. (*Continued*)

Refs	Sensing locations	Sensing platforms	Biomarkers	Applications
[63]	Wrist/ throat/ finger	Textile patch	Blood pulse/ phonation/ body motion	Monitoring of wrist pulse/ phonation/ finger bending, detection of external acoustic vibration/ pressure distribution
[127]	Wrist/ throat/ nape/ finger	Strip	Blood pulse/ phonation/ body motion	Monitoring of wrist pulse/ phonation/ finger bending/neck movement, detection of pressure distribution
[128]	Wrist/ throat/ cheek/ arm/ finger	Patch	Blood pulse/ phonation/ muscle movement/ body motion	Monitoring of radial artery pulse/ phonation/ cheek motion/ forearm muscle movement/ finger flexion and extension

(*Continued*)

Table 2.3 Summary of nanotextiles for multimodal physiological monitoring. (*Continued*)

Refs	Sensing locations	Sensing platforms	Biomarkers	Applications
[124]	Wrist/eye/forehead/philtrum/throat/cheek/elbow joint	Textile patch	Blood pulse/phonation/facial expression/muscle movement/body motion	Monitoring of wrist pulse/cheek bulging/eye blinking/muscle movement of forehead and philtrum during crying and laughing/phonation/chewing/swallowing/coughing/lowering head/elbow bending, detection of external acoustic vibration
[120]	Wrist/throat/eye/knee/finger	Fiber yarn	Blood pulse/phonation/facial expression/muscle movement/body motion	Monitoring of wrist pulse/phonation/eye blinking/finger bending/knee motion
[49]	Chest/arm	Textile patch	ECG/EMG/body motion	Monitoring of ECG/EMG/elbow bending during weightlifting
[46]	Arm	Textile patch	ECG/EMG/body motion	Monitoring of ECG/EMG/elbow bending

(*Continued*)

Table 2.3 Summary of nanotextiles for multimodal physiological monitoring. (*Continued*)

Refs	Sensing locations	Sensing platforms	Biomarkers	Applications
[90]	Wrist/chest	Textile patch	Blood pulse/ respiration	Monitoring of blood pulse/ respiration rate
[86]	Wrist/chest/ throat/ finger/ knee	Skin patch	Blood pulse/ respiration/ phonation/ body motion	Monitoring of wrist pulse/ respiration/ phonation/ finger bending/ knee bending
[84]	Wrist/finger/ abdomen/ throat/ mouth/ neck/ knee/ elbow	Textile patch	Blood pulse/ respiration/ phonation/ muscle movement/ body motion	Monitoring of finger pulse/ wrist pulse/ abdominal breathing/ phonation/ mouth motion/facial expression/ finger bending/ wrist bending/ elbow bending/ knee bending during walking and running
[85]	Wrist/chest/ throat/ finger/ knee	Skin patch	Blood pulse/ respiration/ phonation/ body motion	Monitoring of wrist pulse/ respiration during exercise and sleeping/ phonation/ finger bending/ knee bending

(*Continued*)

Table 2.3 Summary of nanotextiles for multimodal physiological monitoring. (*Continued*)

Refs	Sensing locations	Sensing platforms	Biomarkers	Applications
[87]	Wrist/chest/ throat/ eye/ cheek/ hand	Skin patch	Blood pulse/ respiration/ phonation/ muscle movement/ body motion	Monitoring of wrist pulse/ respiration/ phonation/eye blinking/ facial expression/ hand clenching
[88]	Wrist/ abdomen/ throat/ eye/ finger/ elbow/ knee	Fiber	Blood pulse/ respiration/ muscle movement/ body motion	Monitoring of wrist pulse/ abdominal breathing/ eye blinking/ swallowing/ finger bending/ wrist bending/ elbow bending/ knee bending
[62]	Wrist/chest/ throat/ finger/ knee/eye	Fabric patch	Blood pulse/ respiration/ phonation/ facial expression/ muscle movement/ body motion	Monitoring of wrist pulse/ respiration/ phonation/ eye blinking/ finger bending/ wrist bending/ knee bending, detection of external acoustic vibration

(*Continued*)

Table 2.3 Summary of nanotextiles for multimodal physiological monitoring. (*Continued*)

Refs	Sensing locations	Sensing platforms	Biomarkers	Applications
[129]	Wrist/neck/ finger joint/arm	Skin patch	Wrist pulse/ jugular venous pressure/ body motion	Monitoring of pulse/ jugular venous pressure/ finger bending, detection of acoustic vibration and pressure distribution
[89]	Wrist/chest/ neck/ throat	Skin patch	Blood pulse/ respiration/ jugular venous pressure/ phonation	Monitoring of wrist pulse/ jugular venous pulse/ respiration/ phonation, detection of subtle touch and pressure distribution
[133]	Tooth enamel	Silk film	Exhaled breath/ pathogenic bacteria in saliva	Remote monitoring of respiration/ bacteria in saliva
[134]	Under skin/ stomach/ neck	Thread based patch	Temperature/ strain/pH/ glucose	Monitoring of gastric and subcutaneous pH/strain under various wound conditions

This book chapter will cover the recent progress on nanotextiles for monitoring a broad spectrum of vital signs, as well as other health-relevant parameters, including body temperature, biopotential signals, blood pulse, blood pressure, respiration rate, and biomarkers in biofluids, breath, and body odor. Nanotextiles with single-sensing modalities will be discussed first followed by nanotextiles for multimodal sensing.

2.2 (Bio)Physical Monitoring

Physical biomarkers, such as body temperature, electrophysiological signals, blood pulse and pressure, and respiration, offer important information about the wellness and illness of human body as well as the level of physical activities [2, 18, 19]. Portable and long-term tracking of such signals in home settings greatly benefit the disease diagnosis and possible therapeutic intervention [20, 21]. This section discusses the recent advances in noninvasive and continuous monitoring of physical physiological parameters enabled by wearable nanotextiles.

2.2.1 Body Temperature

Body temperature is one of the basic physiological parameters that require routine monitoring. It is an important indicator of the enzymatic activity involved in metabolism, blood circulation, and immune system and therefore reflects health conditions and body activities [22]. Temperature monitoring provides essential information in the diagnosis of cognitive disorders, circulatory shocks, cardiovascular diseases, cancers, infectious diseases, and other syndromes [2]. Wearable textile sensors can evaluate the body temperature through the detection of skin temperature. The accurate sensing of temperature requires high sensitivity, fast response, high resolution (less than 0.1°C), and sensing range from 25°C up to 40°C [1, 23].

Temperature can be measured based on the thermoresistive effect, pyroelectric effect, and thermoelectric effect. The dominant mechanism for designing textile temperature sensors is the thermoresistive effect. Based on the dependence of resistance on temperature, materials can be divided into two categories. In the first category, the resistance of materials increases with temperature and exhibits a positive temperature coefficient (PTC). In the other category, the resistance decreases with temperature, showing a negative temperature coefficient (NTC). The dependence of resistance on temperature can be expressed by [18].

$$R_T = R_{T_0} \exp \beta \left(\frac{1}{T} - \frac{1}{T_0}\right)$$

where R_T and R_{T_0} are the resistance at temperature T and T_0, respectively. β is the material constant related to the Boltzmann relation $\frac{E}{kT}$ with E and k being the bandgap and Boltzmann constant, respectively. The temperature coefficient of resistance (TCR), which is the percentage change of resistance per degree, is thus given by [18, 24].

$$\alpha_T = \frac{1}{R_T}\frac{dR(T)}{dT} = -\frac{\beta}{T^2}$$

Wearable textile temperature sensors are commonly made into the shape of fibers [25–30] or skin-mountable patches [31, 32]. Various materials, including metallic materials [31, 33] and carbon-based materials [26–29, 34, 35], were adopted to develop thermoresistive temperature sensors. For example, helical rGO fibers with uniform loops and controlled diameters were fabricated (Figure 2.1a), which exhibited a negative TCR in response to a wide temperature range up to 300°C [27]. For wearable thermoresistive temperature sensors, it is challenging to decouple the contribution of temperature-induced resistance changes and strain-induced resistance changes. Novel designs in sensor structures are needed to eliminate the influence of strain. One such temperate sensor was developed using the Kirigami-inspired structure (Figure 2.1b) [36]. The Kirigami pattern effectively reduces the strain applied to the AgNW networks by out-of-plane deformations. The FEA simulation reveals an average tensile strain as low as 0.03% and a maximum strain of 0.56% under 100% tensile strain. As a result, the piezoresistive temperature sensor showed stable temperate sensitivity within 100% tensile strain. The island-bridge strategy was also introduced to fabricate strain-insensitive temperature sensors [32]. As shown in Figure 2.1c, polyaniline NF-based temperature sensors were placed on nonstretchable plastic films (islands) that are connected by stretchable liquid metal interconnections (bridges). Upon stretching, the strain exerted on nonstretchable islands is greatly relieved by the much more stretchable bridges. The temperature sensitivity of 1.0% $°C^{-1}$ and response time of 1.8 s over the range of 15°C to 45°C were demonstrated, which was independent of biaxial strain up to 30% (Figure 2.1d). Of note is that the temperature sensor array adopts an active matrix backplane based

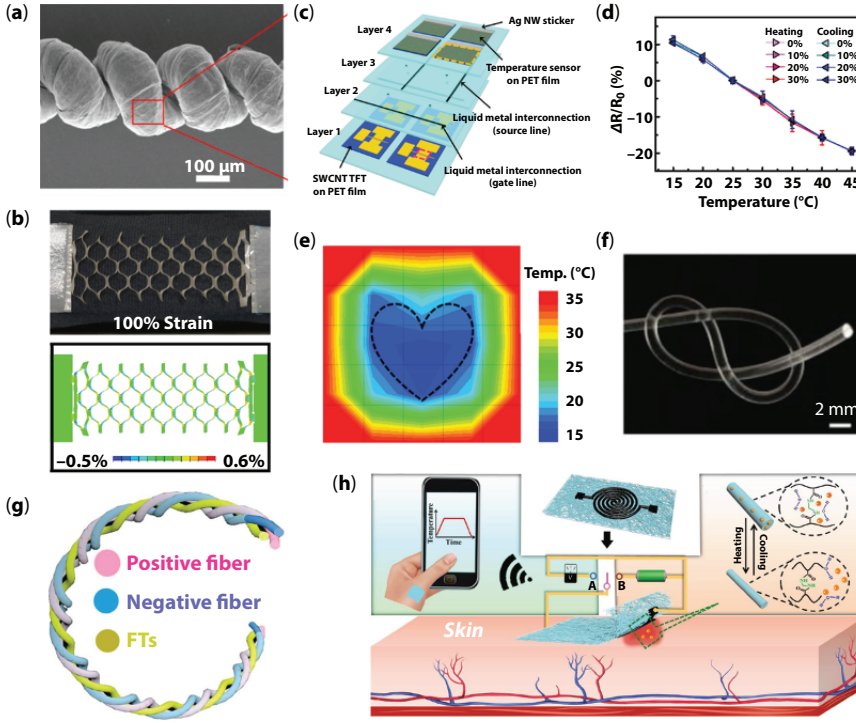

Figure 2.1 Smart nanotextiles for temperature monitoring. (a) An SEM image of the helical rGO fiber for temperature sensing (reprinted from reference [27], with permission of Royal Society of Chemistry). (b) Photograph (top) and FEA simulation (bottom) of the AgNW based temperature sensor with Kirigami structures under 100% tensile strain (reprinted from reference [36], with permission of American Chemical Society). (c) Assembly of a biaxially stretchable active matrix temperature sensor array with stretchable liquid metal interconnections (reprinted from reference [32], with permission of John Wiley and Sons). (d) Temperature responses of the active matrix temperature sensor in (c) under a biaxial strain up to 30% (reprinted from reference [32], with permission of John Wiley and Sons). (e) The temperature sensor array in (c) attached to the palm and the corresponding temperature distribution of the heart-shaped cold water container placed on top (reprinted from reference [25], with permission of John Wiley and Sons). (f) Stretchable optical fibers for temperature sensing (reprinted from reference [32], with permission of John Wiley and Sons). (g) Schematics of the integrated fiber temperature sensors (FTs) and supercapacitors (reprinted from reference [28], no permission is necessary under the terms of Creative Commons CC BY license). (h) A breathable and flexible device that integrates a temperature sensor for wireless temperature monitoring with a screen-printed heater and thermoresponsive materials for on-demand therapy (reprinted from reference [31], with permission of John Wiley and Sons).

on CNT thin-film transistors. The active matrix acts as a switch to address each sensing element, allowing for reduced system power consumption, improved response time, and minimized signal crosstalk among sensors [32, 37]. With such a biaxially stretchable temperature array as the electronic skin, the spatial temperature mapping of the object placed on the palm can be readily detected (Figure 2.1e).

In addition to thermoresistive temperature sensors, efforts have also been devoted to developing optical temperature sensors [25]. Stretchable optical fibers with $NaYF_4$:Yb,Er@$NaYF_4$ core/shell structures (Figure 2.1f) were fabricated via injection and dip coating. The temperature sensitivity can be attributed to the thermally coupled energy states of Er^{3+} and the resulting temperature-dependent emission intensities of $NaYF_4$:Yb,Er@$NaYF_4$ NPs. The temperature sensors can detect the temperature from 25–70 °C, with a sensitivity of 1.8% $°C^{-1}$, resolution of ±0.3 °C, and response and recovery time of 4.5 and 12.5 s, respectively. By placing the optical fibers in the mouth, on the hand, and near the nose, the thermal activities associated with the mouth, hand skin, and during inhale and exhale can be monitored.

The integration of other functionalities to temperature sensors extends the potential range of applications. Figure 2.1g demonstrates the integration of fiber-shaped temperature sensors and asymmetric supercapacitors by twisting a 3D printed temperature-sensitive rGO fiber, an SWCNT/V_2O_5 fiber cathode and an SWCNT/VN fiber anode [28]. The supercapacitor is able to provide a maximum operating voltage of 1.6 V, sufficient to supply the voltage needed (1 V) for the temperature sensor. The integrated temperature sensor exhibits a temperature sensitivity of 1.95% C^{-1} for the temperature range of 30–80°C.

Elevated temperature can be a sign of inflammation or infection. Integrating temperature-sensitive elements with heating components enables temperature sensing and feedback anti-infection therapy [31]. In a representative work shown in Figure 2.1h, the device was built upon an electrospun breathable thermoresponsive polymer nanomesh film. Conductive Ag patterns were screen printed on the nanomesh to act as heaters and moxifloxacin hydrochloride (MOX) was loaded on the fibers to perform thermoresponsive release of antibiotics for inhibiting the growth of bacteria. The combined breathability, flexibility, stability in different mediums (i.e. air, NaOH solution, phosphate buffered solution (PBS), and cell culture medium), together with the real-time temperature sensing and on-demand therapy provide an effective platform for wound site monitoring and treatment.

2.2.2 Biopotential Signals

Biopotential sensors monitor bioelectrical potentials that originate from the propagation of the action potential through body's excitable cells [38]. Through noninvasive measurements of minute potential difference on the skin surface, biopotential sensing provides insights about the function of organs, including heart, muscle, eye, nerve, and brain. For instance, electrocardiography (ECG) measures the electrophysiological patterns generated by depolarization and repolarization of the cardiac muscle during cardiac cycles. Electromyography (EMG) detects the electrical activity of skeletal muscles in response to nerve stimulation. Electroencephalography (EEG) records the activity of the brain and is widely used to diagnose epilepsy, stroke, and sleep disorders. Electroretinography (ERG) monitors the electrical variations in the retina in response to stimuli.

Biopotential sensing is typically implemented by placing electrodes on the skin surface to capture the potential changes in a noninvasive manner. While the most commonly used electrodes in the hospital setting are pregelled electrodes, these electrodes face challenges for long-term monitoring due to the dehydration over time and potential dermal irritation and allergic reactions during prolonged wear [39, 40]. In addition, the high cost in hospital-centered testing greatly limits the comprehensive monitoring of electrophysiological conditions. Dry electrodes address the problems by exploiting gel-free electrodes made of CNTs [41–43], rGO [44, 45], AgNWs [46–48], and nanofibers coated with conductive materials [49–51].

Among a variety of biopotential sensing modalities, the most extensively studied one so far is ECG [41–46, 49, 51]. ECG plays an indispensable role in the early diagnosis and management of cardiovascular diseases. The most common location for placing textile-based ECG electrodes are arms, wrists, or fingers with lead I configurations. The electrode-skin impedance is commonly measured to evaluate how effective electrical variations are transferred from human body to electrodes, typically by placing a pair of electrodes on the skin with the impedance between electrodes measured [7]. In an example of dry textile ECG electrodes, nylon fibers were dip-coated with rGO to render an electrical conductivity of 4.5 S/cm (Figure 2.2a) [44]. The electrode-skin impedance is slightly higher than that of commercial Ag/AgCl pre-gelled electrodes. A high correlation of 97% was achieved between the signals obtained using textile electrodes and Ag/AgCl electrodes, indicating high-quality ECG recordings using the rGO/nylon electrodes. In another work, rGO was inkjet printed onto organic NPs modified textiles [45]. The surface modification by organic

NPs increases the water contact angle and inhibits the liquid penetration on textiles during printing. By placing left and right fingers on printed textile electrodes, ECG patterns were obtained, and the heartbeat can be derived from the spacing of R peaks. Although the textile electrodes survived ten washing cycles, a significant increase in the resistance was seen with increasing the number of washing cycles.

Besides ECG sensing, the dry textile electrodes can also be used for EMG/EEG sensing as well as electrodermal activity (EDA) monitoring. Figure 2.2b shows the fabrication of conductive SWCNT/poly(vinylidene fluoride-co-hexafluoropropylene) (PVdF-HFP) nonwoven fabrics by a blow-spinning process [41]. With nonwoven fabric electrodes, ECG and heartbeat during running and relaxing states were measured using three electrodes attached on the left arm, right arm, and left leg, respectively. EMG signals related to fist clenching were measured by placing two electrodes on the forearm. For EEG signals, three electrodes were attached to the frontal pole 1, frontal 7, and left earlobe locations. EEG patterns with different frequency characteristics were observed corresponding to different brain activities during napping, waking up from napping, and solving math problems. At last, the electrodes can be used for recording EDA with two electrodes placed on the volar surface of distal phalanges. EDA measures fluctuations of the electrical conductance of skin due to the sweat gland activity, reflective of emotional arousals.

The function of nanotextiles can be further extended beyond skin surface electrodes. To evaluate the functionality of retina, dry electrodes that can be integrated with contact lenses and interfaced with eyes were developed. As illustrated in Figure 2.2c [50], the transparent device was built upon the commercial contact lens, where Au was sputtered on the NF-based nanomesh as the conductor. Poly(3,4-ethylenedioxythiophene) (PEDOT)/poly(styrene sulfonate)(PSS) was electrochemically deposited to improve the stretchability and wettability of the nanomesh. A water contact angle of ~12.2° ensures good tear spreading, important for ensuring a conformal contact between the contact lens and cornea for accurate sensing. Gas permeability of electrodes is an important aspect for long-term electrophysiological monitoring [52, 53]. Thanks to the breathability of the nanomesh, the contact lens device maintained a similar high oxygen permeability to pure hydrogel lenses. Negligible corneal abrasion or irritation was observed in the rabbit eyes that worn the contact lens for 12 hours, validating the compatibility required for long-term wear. Full-field ERG recordings, including scotopic ERG, photopic ERG, and 30 Hz flicker ERG responses, achieved by the contact lens device, showed comparable signal quality to that recorded by commercial Jet electrodes.

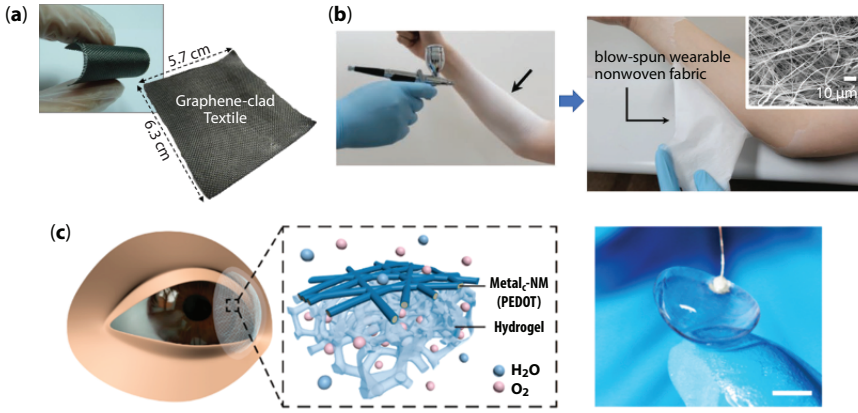

Figure 2.2 Smart nanotextiles for biopotential monitoring. (a) Photograph of rGO-coated nylon fibers for ECG sensing (reprinted from reference [44], with permission of Elsevier). (b) Photographs showing the blow spinning of PVdF-HFP nonwoven fabric onto the skin. The inset shows the SEM image of the blow-spun nonwoven fabric (reprinted from reference [41], with permission of John Wiley and Sons). (c) Schematics (left) and photograph (right) of the gas-permeable and transparent hydrogel contact lens device for ERG recordings. Scale bar, 5 mm (reprinted from reference [50], with permission of American Chemical Society).

2.2.3 Blood Pulse

The heart is one of the most vital organs in human body that closely relates to one's overall health. Pulse wave represents one of the most direct and crucial signals that indicate the health conditions of the heart and cardiovascular system. Comprehending pulse waves in real time is beneficial to preventing many physiological diseases, such as heart attack and stroke [54, 55]. Abnormal pulse waveforms have been considered as important symptoms for early diagnosis of the physiological and pathological status of the cardiovascular system [56].

Intensive studies have been performed focusing on long-term and noninvasive blood pulse monitoring. Commercial techniques for measuring pulse waves mostly require a hand cuff (Korotkoff sound method or oscillometric type) that may cause discomfort to patients during testing. Besides, these devices have disadvantages including high fabrication costs, reliance on batteries, and poor portability [57, 58]. New technologies for measuring pulse waves, such as photoplethysmography (PPG) and piezoelectric pulse transducer (PPT), have been developed. However, such measurements are indirect, highly dependent on empirical models [59].

Additionally, interferences, such as body movements and vibrations, can greatly affect PPG measurements.

Novel techniques for long-term and real-time monitoring of pulse waves are enabled by wearable sensors. Such sensors can be attached to human body (e.g. wrist, neck) to detect subtle strain or pressure on human skin induced by vessel pumping. As an example, a graphene/silk pressure sensor was developed that adopted the thermal reduction process to achieve 3D structures on the soft silk substrate (Figures 2.3a and 2.3b) [60].

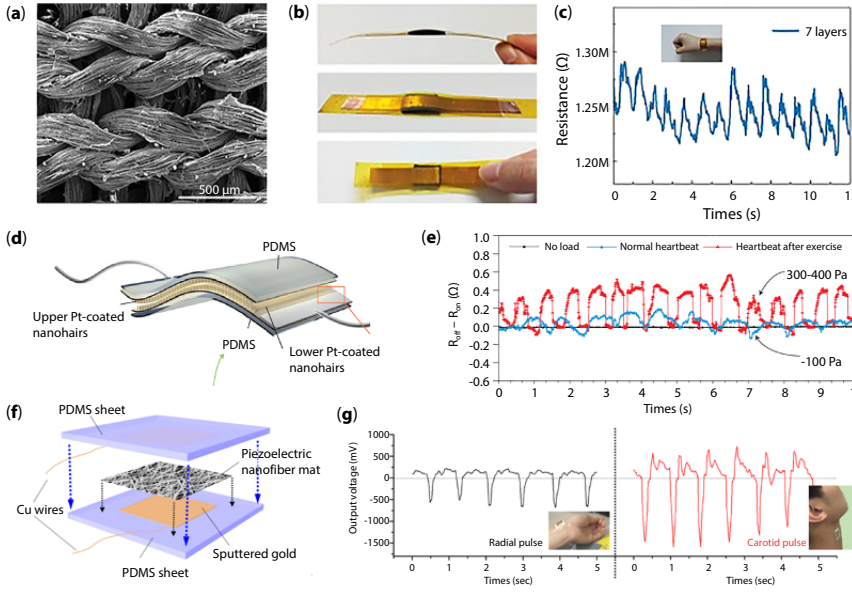

Figure 2.3 Smart nanotextiles for blood pulse monitoring. (a) SEM image of the graphene/silk pressure sensor (reprinted from reference [60], with permission of AIP Publishing). (b) Photographs of graphene/silk pressure sensor wrist bands (reprinted from reference [60], with permission of AIP Publishing). (c) Resistance change of the graphene/silk pressure sensor indicating the pulse wave. The inset photograph shows the sensor attached to the wrist (reprinted from reference [60], with permission of AIP Publishing). (d) Schematics of the interlocked fiber array based piezoresistive sensor (reprinted from reference [67], with permission of Springer Nature). (e) Real-time sensor output for pulse monitoring under normal condition and after exercises using the sensor in (d) (reprinted from reference [67], with permission of Springer Nature). (f) Schematics showing the sandwich structure of electrospun nanofiber enabled stretchable piezoelectric sensors (reprinted from reference [68], with permission of American Chemical Society). (g) Real-time sensor output for radial and carotid pulse monitoring by putting sensors in (f) on the wrist and neck respectively (reprinted from reference [68], with permission of American Chemical Society).

The pressure sensor achieved a high sensing range (up to 140 kPa) with a sensitivity of 0.4 kPa^{-1}. Due to the use of silk substrates, such pressure sensors can be easily integrated into existing knitted textile products. The sensor can be used as an arterial pulse sensor by putting on the wrist (Figure 2.3c). Similar combinations of conductive materials and fibers/yarns/fabrics/textiles have been intensively studied as applicable sensing materials for pulse waves [61–66].

Besides typical piezoresistive sensors as discussed above, sensors based on contact resistance can also be utilized for wearable blood pulse sensing. A novel interlocking structure of two arrays of conductive Pt-coated NFs (Figure 2.3d) has been reported for the sensing of pressure, shear, and torsion [67]. When two arrays are under stretching, the effective contact area changes, leading to the change of electrical resistance. The sensing mechanism was tested to be reversible and extremely sensitive with a gauge factor of 11.45 for pressure, 0.75 for shear, and 8.53 for torsion. The sensor was attached above the artery of the wrist to monitor the pulse waves in normal conditions and after exercise in real-time (Figure 2.3e).

Another strategy of measuring pulse wave is by using piezoelectric materials. A piezoelectric sensor was fabricated by assembling poly-(vinylidene fluoride-trifluoroethylene) (PVDF-TrFE) NFs on elastomer films (Figure 2.3f) [68]. Electrospinning was adopted to obtain a mat structure with good piezoelectric properties and mechanical durability. By putting onto the wrist and neck, radial and carotid pulses were measured respectively as shown in Figure 2.3g. Similar structures using PVDF-HFP NFs have been reported as a wrist pulse sensor for heart rate monitoring [69].

2.2.4 Blood Pressure

With the heart being the main pump of human body, another crucial parameter that characterizes the pump is 'Blood Pressure'. Blood pressure represents the force of heart muscles that promotes the blood flow. Maintaining a certain range of blood pressure levels is of paramount importance. A higher (hypertension) or lower (hypotension) than normal blood pressure indicates malfunctions of the cardiovascular system. The blood pressure can be categorized as the systolic blood pressure (SBP) and the diastolic blood pressure (DBP) [70]. SBP characterizes the contracted status of the heart while DBP represents the relaxed status [71–73]. Wearable blood pressure sensors for long-term monitoring have attracted attention for the early prevention of heart diseases, such as stroke, coronary artery diseases, and myocardial ischemia.

Figure 2.4a presents a CNT and graphene based transparent bending-insensitive pressure sensor [74]. The sensor was fabricated by an electrospinning process to disperse nanomaterials into the fluorinated copolymer, which serves as a nanofiber matrix. An important feature of the pressure

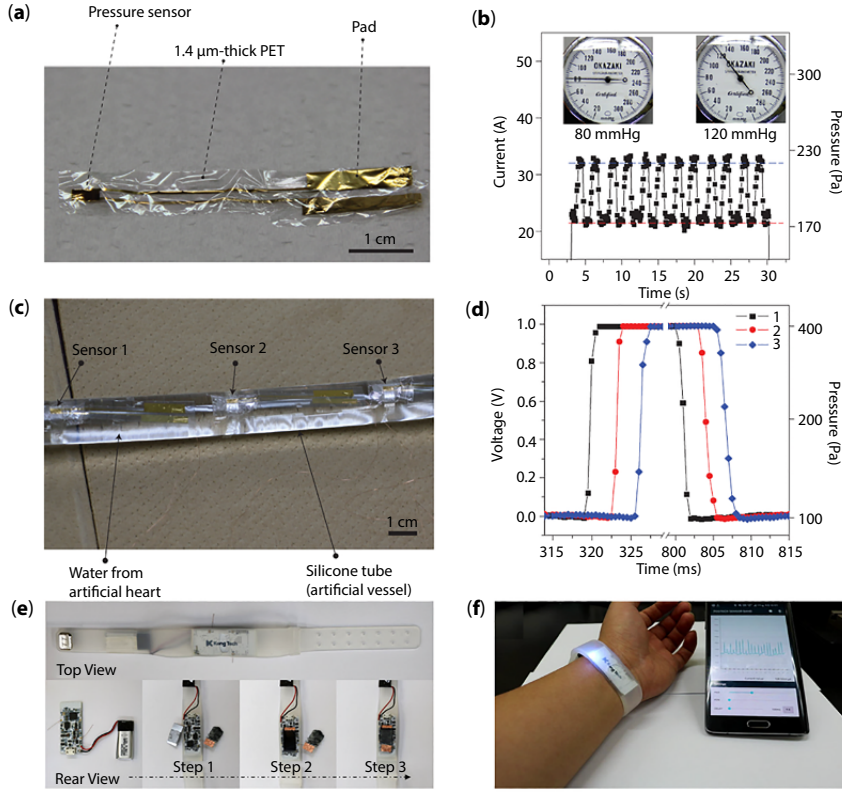

Figure 2.4 Smart nanotextiles for blood pressure monitoring. (a) Photograph of a CNT and graphene enabled pressure sensor (reprinted from reference [74], with permission of Springer Nature). (b) Cyclic test of the sensor attached to an artificial blood vessel under pressure ranging from 80 to 120 mmHg (reprinted from reference [74], with permission of Springer Nature). (c) Photograph of an artificial blood vessel with three sensors attached for measuring the pressure propagation (reprinted from reference [74], with permission of Springer Nature). (d) Response of three pressure sensors on the artificial blood vessel under one pressure wave (reprinted from reference [74], with permission of Springer Nature). (e) Top and rear-view photographs of a PVDF-HFP/PEDOT enabled pressure sensor embedded in a wrist band (reprinted from reference [75], no permission is necessary under the terms of Creative Commons CC BY license). (f) Photograph showing the wireless monitoring of blood pressure using the PVDF-HFP/PEDOT enabled pressure sensor and smartphone (reprinted from reference [75], no permission is necessary under the terms of Creative Commons CC BY license).

sensor is the small sensitivity to the bending strain endowed by the nanofibrous structure, which is crucial for blood pressure sensing. Experimental results revealed the capabilities of detecting the cyclic change in pressure (50 Pa) (Figure 2.4b). To demonstrate the usability, the sensor was applied to an artificial blood vessel (Figure 2.4c). Moreover, three pressure sensors were attached to the artificial blood vessel and the pulse wave propagation was captured by comparing the time delay in three output signals (Figure 2.4d).

In another work, a highly sensitive piezoelectric pressure sensor based on the electrospun PVDF-HFP/PEDOT mat was proposed [75]. The key fabrication method includes 3D electrospinning and vapor deposition polymerization. The unique 3D membranes enable a greatly enhanced sensitivity (13.5 kPa^{-1}) as compared to sensors with conventional 2D structures. The minimum detection range is as low as ~1 Pa and cyclic tests showed the repeatability of over 10,000 times. A wearable wrist band containing the pressure sensor was tested on the wrist to monitor blood pressure (Figure 2.4e). A wireless system with a user interface on the smartphone for displaying real time blood pressure was developed and demonstrated (Figure 2.4f).

Besides direct measurement using pressure sensors, blood pressure (P) can be obtained indirectly by measuring the pulse wave velocity (PWV) in the artery [76]. The Rogers group established the correlation between the blood pressure and PWV [77]:

$$P = \alpha \mathrm{PWV}^2 + \beta = \alpha \frac{L^2}{\Delta t^2} + \beta$$

where L indicates the pulse arrival distance, Δt indicates the pulse arrival time, α and β are parameters related to material properties and geometry of the artery. Based on this formula, ECG electrodes and pulse rate sensors as discussed in Section 2.2.2 and 2.2.3 can be promising in developing blood pressure sensors. For instance, with the ECG electrodes and pulse rate sensor placed with a distance of L, noninvasive and cuffless monitoring of blood pressure can be achieved by measuring the time interval Δt between the ECG R peak and the pulse wave [78, 79].

2.2.5 Respiration Rate

Among various vital signs, respiratory activity is important as the breathing pattern yields essential information about the general health and condition

of patients [80]. Abnormalities in breathing can be indicators of many illnesses including asthma, anemia, sleep apnea, panic attacks, heart failure, or chronic obstructive pulmonary diseases [81].

Traditional methods of monitoring the respiration rate include pneumography [82], which measures circumference change of the chest during breathing, and pulse oximetry [83], which measures the blood oxygen saturation using a device clamping on locations, such as fingers and toes. Both methods cause interference to normal body activities and are unsuitable for long-term monitoring. Since nanotextile-based sensors are flexible and lightweight in comparison to rigid instruments, they have been pursued as new platforms for wearable respiration monitoring.

Highly sensitive wearable strain [62, 84–88] or pressure [89] sensors can monitor the respiration by tracking the mechanical deformations generated during respiratory activities on the chest [62, 85–87, 89, 90] or abdomen

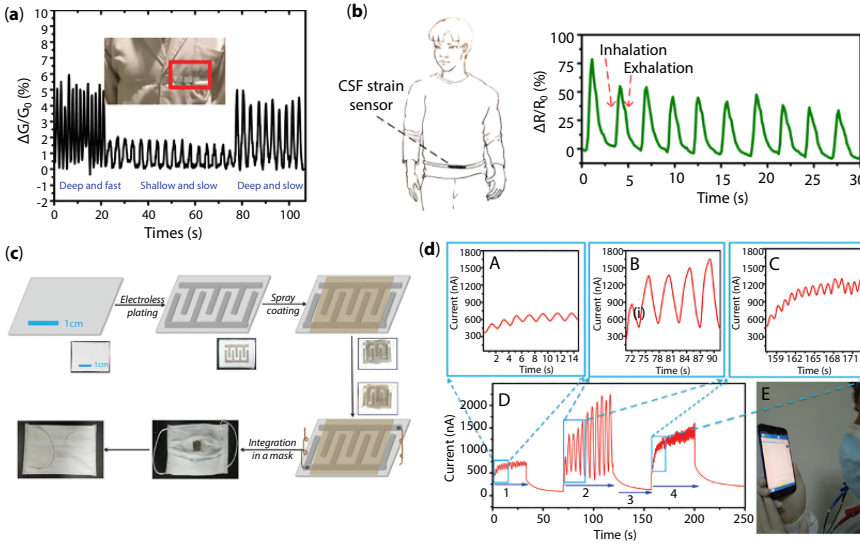

Figure 2.5 Smart nanotextiles for respiration rate monitoring. (a) Respiration monitoring under different conditions by placing CNT/nonwoven fabric sensors on the chest (reprinted from reference [90], with permission of Royal Society of Chemistry). (b) Respiration monitoring by placing CNT core-sheath fibers on the abdomen (reprinted from reference [88], with permission of American Chemical Society). (c) Fabrication process of a GO/silk humidity sensor and the integration with the face mask (reprinted from reference [91], with permission of Royal Society of Chemistry). (d) Respiration monitoring under different scenarios (normal/deep/fast breathing) using the GO/silk humidity sensor integrated with a face mask (reprinted from reference [91], with permission of Royal Society of Chemistry).

[84, 88]. These nanotextile sensors are typically based on the piezoresistive mechanism, where the respiration pattern triggers the change in the resistance of sensors. Figure 2.5a illustrates a wearable piezoresistive respiration sensor in which CNTs were incorporated onto the nonwoven fabric using ultrasonic nanosoldering [90]. The sensor can survive a vigorous washing process due to the strong adhesion of CNTs to polymer fibers. By attaching the sensor on the chest, monitoring of respiration under different conditions was performed. Different respiration rates and patterns were captured in real time. Figure 2.5b presents the respiration sensing by placing a strain sensor on the abdomen [88]. The sensor was enabled by CNT based core–sheath fibers prepared via a coaxial wet spinning technique. Repeated resistance changes during inhalation and exhalation were observed, suggesting a respiration rate of around 20 breaths per minute.

Another way of monitoring respiration is to detect the transient difference in moisture when inhaling and exhaling air. A silk-based humidity sensor for respiration monitoring has been reported [91]. As shown in Figure 2.5c, the sensor was fabricated by electroless plating of conductive electrodes and spray coating of a GO layer. By integrating with a face mask, the humidity sensor could accurately detect respiration patterns under different scenarios including normal, deep, and fast breathing (Figure 2.5d). Comparing with deformation-based respiration sensors as mentioned above, humidity sensors reduce the discomfort brought to the users to a minimum. Additionally, humidity sensors are free from interferences from body movements.

2.3 (Bio)Chemical Monitoring

Biochemical parameters are critically relevant to health status and body activities, largely due to their close relations to the physical, chemical, and biological aspects of human body [92, 93]. Although these biomarkers can be precisely accessed by conventional blood tests, noninvasive detection is in demand for continuous health monitoring [20, 94]. This section discusses noninvasive biochemical monitoring from biofluids secreted by human body (e.g. sweat, tear, saliva) and gases emanated from human body (e.g. breath, body odor).

2.3.1 Biofluids

Biofluids, such as blood, sweat, tear, saliva, interstitial fluid, and urine, are abundant in physiologically relevant chemical constituents, which can

provide diagnostic vehicles to quantify key biochemical cues [94, 95]. In particular, naturally excreted sweat and tear fluids are attractive due to the ease of collection and sampling. Sweat possesses rich information that can be used to probe metabolism, nutrition, physical performance, dysfunction, and diseases [96]. Recent progress has been made to analyze metabolites, electrolytes, and pH in sweat with nanotextile sensors [97–102].

One representative example is an electrochemical fabric platform by weaving CNT fibers functionalized with different active materials for a variety of biomarkers (Figure 2.6a) [102]. The flexible electrochemical fabric and a flexible fiber-shaped lithium-ion battery were assembled into a garment. Real-time and wireless analysis of glucose, Na^+, K^+, Ca^{2+}, and pH during running was realized. The accuracy of the *in situ* sweat analysis was cross-validated against the *ex-situ* measurement on the collected sweat samples performed by commercial sensors. Figures 2.6b and 2.6c exemplify another work of textile-based electrochemical sensors for detecting sweat ions, which were enabled by screen-printed CNT electrodes and polyurethane (PU)-based ion-selective membranes [103]. Highly stretchable CNT inks and serpentine patterns ensure the robustness against stretching up to 100% strain, repeated bending, and washing. The printed sensor array is able to detect both Na^+ and K^+ ions with a detection limit of $10^{-4.9}$ M, sensitivities of 59.4 mV/log [Na^+] and 56.5 mV/log [K^+], over the range of 10^{-4} M to 10^{-1} M. The sensor could be fabricated into different form factors including underwear, watch straps, and elastic band.

Sensing systems without external power connections represents a technological advance for wearable health monitoring. Self-powered sensors can be realized by employing intrinsically self-powered sensing mechanisms, such as triboelectricity and piezoelectricity, or by incorporating wearable energy harvesters [4, 15]. Biofuel cells are promising as self-powered biochemical sensors that convert the biochemical energy in biofluids into electrical energy through reduction-oxidation reactions [21, 104]. A noteworthy example of such textile-based self-powered sensors was reported by the Wang group (Figure 2.6d) [105]. Stretchable enzymatic biofuel cells were enabled by printing stretchable inks into serpentine patterns that can maintain structural integrity under repeated mechanical deformations. The stretchable biofuel cells exhibit increased power density with glucose/lactate concentrations up to 50 and 20 mM. The cells generated maximum power densities of 160 and 250 μWcm^{-2} with the open-circuit voltage of 0.44 and 0.46 V for glucose and lactate cells, respectively. The on-body experiment performed during cycling demonstrated the capabilities of energy scavenge from the lactate in sweat, noninvasive sensing of

the lactate concentration, and wireless visualization of the result on the smartphone.

Tear fluids contain a variety of chemical biomarkers relevant to ocular conditions, such as metabolites, enzymes, proteins, salts, lipids, and immunoglobin [94, 106, 107]. Aside from sweat, tear serves an alternative diagnostic fluid, which can be readily obtained in a natural way. The contact lens provides a convenient platform to interface with tears for continuous sensing. An impressive example of electrochemical sensing from tear fluids is shown in Figure 2.6e [108]. The proposed contact lens device comprises a wireless power transfer module, a glucose sensor, and a LED display pixel. Ultralong electrospun Ag NFs were adopted as transparent and stretchable conductors. Island-bridge design was exploited to ensure the high stretchability of the device. The rectifier, glucose sensor, LED pixel were placed on the reinforced regions serving as islands, while the transparent antenna

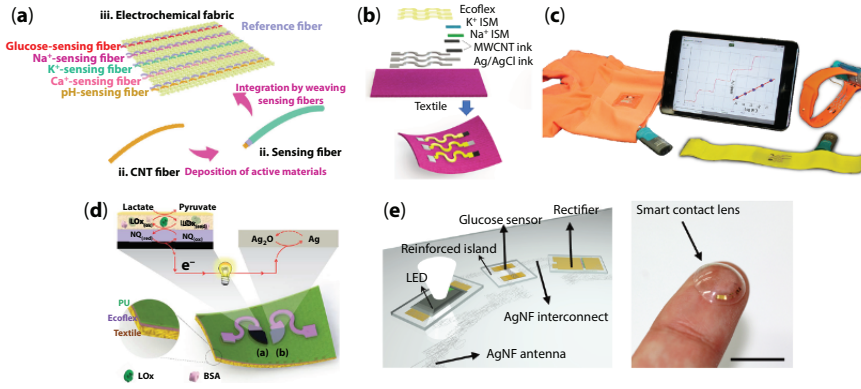

Figure 2.6 Smart nanotextiles for biochemical monitoring in body fluids. (a) Schematics of the electrochemical fabric by weaving functionalized CNT sensing fibers (reprinted from reference [102], with permission of John Wiley and Sons). (b) Schematics of the structure of the textile-based stretchable multi-ion sensor (reprinted from reference [109], with permission of John Wiley and Sons). (c) Photographs showing different form factors (i. e. underwear, watch straps, and elastic band) of the sensor array and a tablet for displaying real-time potassium levels obtained wirelessly from the sensor printed on the underwear (reprinted from reference [103], with permission of John Wiley and Sons). (d) Schematics showing the component and self-powered sensing mechanism of the stretchable lactate biofuel cell (reprinted from reference [105], with permission of Royal Society of Chemistry). (e) Schematics (left) and photograph (right) showing the smart contact lens for glucose sensing and visualization, where the rectifier, LED pixel, and glucose sensor were placed on the reinforced regions while the transparent and stretchable antenna and interconnects were placed on the elastic region. Scale bar, 1 cm (reprinted from reference [108], with permission of The American Association for the Advancement of Science).

and interconnects based on Ag NFs were placed on the elastic region serving as bridges. The contact lens can detect and visualize the glucose concentration in tears wirelessly in real-time; AC power can be transmitted wirelessly through the inductive coupling and rectified to power the LED pixel. Once the glucose concentration increases, the decrease in the sensor resistance leads to a decrease in the bias applied to the LED pixel. This way, the glucose level above a threshold will be wirelessly monitored and reflected in the off state of the integrated LED display.

2.3.2 Breath and Body Odor

In addition to monitoring respiration rate as discussed in Section 2.2.5, monitoring biochemical characteristics of the respiration, such as breath humidity, volatile organic compounds (VOCs), and disease-specific biomarkers in exhaled breath, is of increasing interest for the diagnosis of diseases. For example, the concentration of emanated ethanol, acetone, trimethylamine, and ammonia can be correlated with hepatic steatosis, diabetes, uremia, and kidney disorders, respectively [109, 110].

Recent efforts on nanotextiles for breath humidity sensing include the application of MoS_2-coated optical fibers [111], GO-coated silk fabric [91], MXene/AgNW decorated silk [112], and nitrogen-doped rGO fibers [113]. MXene/AgNW decorated silk, for example, detects the mouth and nose breath through the change in resistance [112]. The decorated silk textile also possesses superior electromagnetic interference shielding performance and superhydrophobicity. In another work, humidity sensors based on nitrogen-doped and Pt NPs functionalized rGO fibers yield a relative humidity (RH) sensing range of 6.1–66.4% and a sensitivity of 4.51% (66.4% RH) [113]. As described in Figure 2.7a, a portable breath humidity platform was constructed by integrating the sensor with a flexible printed circuit board for wireless data communication to a smartphone. An increased resistance change was observed for higher breath humidity.

The detection of gaseous biomarkers in exhaled breath requires gas sensors with high sensitivity and selectivity in a humid environment. In a representative work, electrospun WO_3 NFs were leveraged for sub-ppm level gas sensing [114]. The gas sensor provides high sensitivity, superb selectivity, and fast response. By employing sensor arrays composed of WO_3 NFs functionalized with three types of catalysts (i.e. Pt, Pd, and Rh NPs), ten different biomarkers can be clearly identified and detected using the principal component analysis (Figure 2.7b).

In addition to exhaled gas in the breath, other body odors, such as urine odor, can also be indicative of diseases. Figures 2.7c and 2.7d highlight an

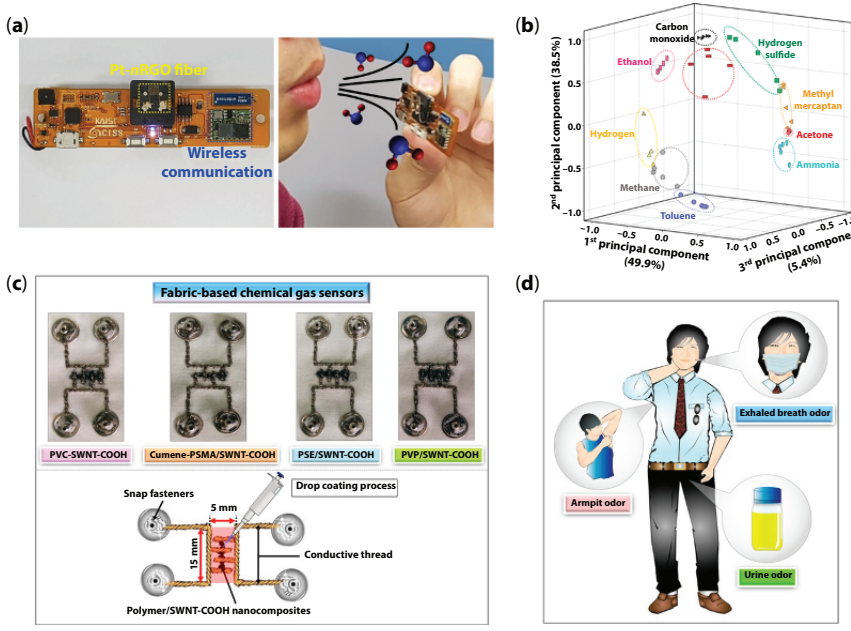

Figure 2.7 Smart nanotextiles for biochemical monitoring in breath and body odor. (a) Photographs showing the portable breath humidity sensor based on Pt functionalized rGO fibers (reprinted from reference [113], with permission of John Wiley and Sons). (b) Pattern recognition of 10 different biomarkers at different concentrations using principal component analysis (PCA) and mesoporous WO_3 NFs functionalized with catalytic Pt, Pd, and Rh NPs (reprinted from reference [114], with permission of American Chemical Society). (c) Photographs (top) and schematic (bottom) of gas sensors enabled by coating polymer/functionalized-SWNT nanocomposites onto embroidered conductive threads (reprinted from reference [115], no permission is necessary under the terms of Creative Commons CC BY license). (d) Schematics showing the detection of VOCs in different body odors (reprinted from reference [115], no permission is necessary under the terms of Creative Commons CC BY license).

electronic nose composed of four gas sensors for the detection of different body odors [115]. The wearable electronic nose exploits four different polymer/SWNT-COOH nanocomposites, which were coated onto interdigitated electrodes prepared by embroidered conductive threads. With principal component analysis, the electronic nose can be used for detecting VOCs, such as ammonium hydroxide, ethanol, pyridine, triethylamine, methanol, and acetone. The electronic nose could distinguish the body odors between two volunteers through the analysis of VOCs from urine, armpit, and exhaled breath.

2.4 Multimodal Monitoring

Multimodal monitoring and correlation of different physiological parameters provide a more comprehensive insight into personal health as compared to nanotextile sensors with single functions, allowing for more efficient assessment and more informed disease management. Multimodal monitoring can be achieved by employing sensors with multifunctional sensing capabilities or by integrating different sensors into a multisensory platform. This section discusses the recent progress on this front.

2.4.1 Multimodal Monitoring of Physical Biomarkers

Being conformal, lightweight, and unobtrusive, nanomaterial/textile integrated strain and pressure sensors can be applied to monitor many health and activity related signals, as schematically shown in Figure 2.8 [84]. For instance, in addition to detecting blood pulse, piezoresistive sensors can also be put onto the wrist, elbow, finger, or knee joints to track various human motions. Conductive materials, such as carbon black [116], carbonized silk/cotton/woven [62, 117, 118], CNTs [63], graphene [119], GO [91], AgNWs [120], are often combined with existing textile/fabric/yarns to form the strain sensing elements. Analysis of body motions is beneficial to the assessment of body activities and the diagnosis of epilepsy, stroke, nervous system diseases, Parkinson's disease, and sports injuries [46, 121–123]. Another application of strain and pressure sensors is to sense muscle movement and facial expressions by detecting skin movement on different locations, such as forehead, cheek, or philtrum [116, 120, 124]. When put onto the vibrating throat, mechanical sensors can also be used to monitor vocal vibrations when the subject makes different pronunciations [61–63, 66, 117, 125–128].

Multimodal sensing of blood pulse and respiration rate, together with diverse other physical signals, can be readily obtained by attaching strain sensors to the skin surface [85–90]. In particular, recently reported rGO textile-based strain sensors were fabricated through a simple dip-coating process [84]. With sensors attached to the finger, wrist, elbow, knee, abdomen, throat, and mouth (Figure 2.8), both large deformations related to finger, wrist, elbow, and knee bending, and subtle deformations associated with blood pulse, abdominal breathing, phonation, facial expression, muscle movement are monitored. Pressure sensors based on carbonized silk NFs [89] and strain sensors based on crisscross interlaced graphene woven fabrics [129] were developed for concurrent sensing of blood pressure,

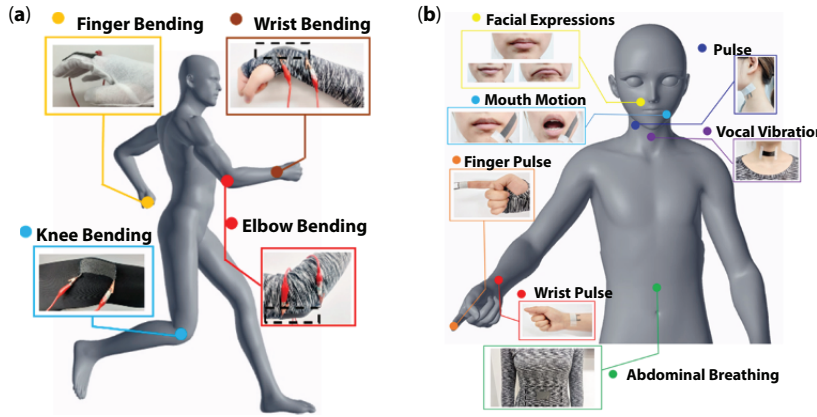

Figure 2.8 Smart nanotextiles for multimodal monitoring of skin deformation associated physical biomarkers. (a) Schematics showing the multifunctional monitoring of different body motions using the wearable textile strain sensor (reprinted from reference [84], with permission of American Chemical Society). (b) Schematics showing the multifunctional monitoring of pulse, respiration, facial expression, muscle movement, and vocal vibration using the wearable textile strain sensor (reprinted from reference [84], with permission of American Chemical Society).

blood pulse, and/or respiration. Figure 2.9a presents the sensing of wrist pulse and jugular venous pressure using the graphene woven fabrics [129]. The sensitivity of the strain sensor is sufficient to clearly identify the characteristic percussion (P), tidal (T), and dicrotic (D) waves in the wrist pulse and A wave, X decent, C wave, V wave, and Y decent in the biphasic waveform of the jugular vein. Additionally, these strain and pressure sensors are applicable for resolving the external sound vibration and/or spatial resolution of touch and pressure.

Figure 2.9b presents an effort to realizing the multifunctional sensing of body temperature and mechanical signals using skin-inspired, layered sensors [130]. The top light/temperature sensors emulate the epidermis, the middle pressure sensor mimics the dermis, and the bottom temperature sensor is inspired by the hypodermis. The wrist temperature, blood pulse, as well as external pressure and infrared light illumination can be detected with negligible interference between different sensing modalities. In another work, in addition to thermoresistive temperature and piezoresistive strain sensing capabilities, the application of graphene doped porous PU fibers adds a self-cooling function to the sensor, taking advantage of the high infrared radiation transparency [131]. The integrated smart sportswear enables the monitoring of vital signs (e.g. body temperature, blood

pulse, and respiration) as well as various muscle movement and body motions (e.g. swallowing, phonation, stretching, walking, chest expanding, finger bending, side twist).

Apart from offering more comprehensive monitoring of physiological parameters, the correlation of electrophysiological variations and body motions provides a possible way to reduce motion artifacts present in biopotential signals using the collected motion signals [46, 49, 132]. Figures 2.9c–e exemplify AgNW based multifunctional textiles, which incorporate four dry electrodes for ECG and EMG sensing, a capacitive strain sensor for motion tracking, and a wireless heater for wearable thermotherapy [46]. The combination of compliant nanomaterials, deformable structures, and scalable laser scribing patterning and heat press lamination processes results in mechanically and electrically robust devices without compromising the stretchability, wearability, and washability of textiles. Similar integration of ECG/EMG sensing and motion tracking capabilities in

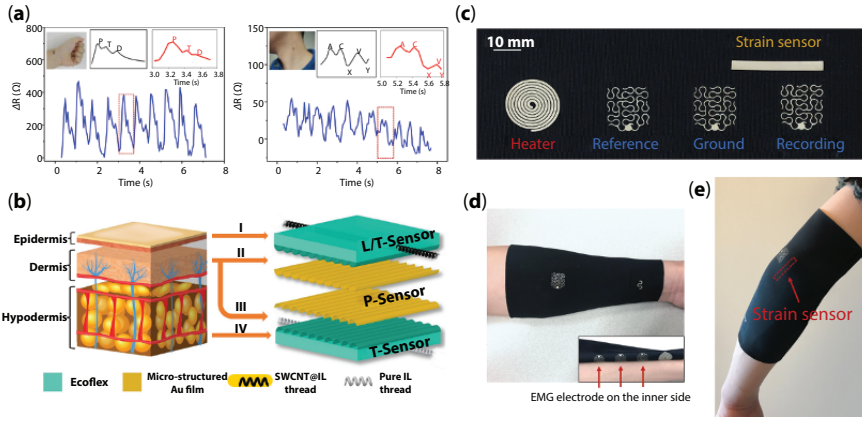

Figure 2.9 Smart nanotextiles for multimodal monitoring of physical biomarkers. (a) Multifunctional monitoring of wrist pulse (left) and jugular venous pressure (right) by graphene woven fabric-based strain sensors (reprinted from reference [129], with permission of American Chemical Society). (b) Schematic illustration of skin-inspired multifunctional sensors. L/T-Sensor: Light/Temperature sensor, P-Sensor: Pressure sensor, T-Sensor: Temperature sensor fibers (reprinted from reference [130], with permission of John Wiley and Sons). (c) Integrated textile patch consisting of four dry electrodes (three are in the front, one in the back), a capacitive strain sensor, and a wireless heater for sports applications (reprinted from reference [46], with permission of American Chemical Society). Photographs showing the placement of the textile patch for (d) EMG sensing and (e) elbow bending tracking (reprinted from reference [46], with permission of American Chemical Society).

electronic textiles was achieved by the application of nanofiber reinforced Ag composites and the introduction of buckling structures [49].

2.4.2 Multimodal Monitoring of Physical and Chemical Biomarkers

Progress has also been made to achieve multimodal sensing of physical and biochemical parameters. The McAlpine group proposed a graphene/silk platform that can interface with the tooth for monitoring respiration patterns and bacteria in saliva down to the single bacterium level [133]. As schematically illustrated in Figure 2.10a, the platform consists of a sensing element based on functionalized graphene and integrated wireless power and readout element based on an interdigitated capacitor in connection with an inductive coil antenna. The exhaled breath or the concentration of bacteria (*H. pylori*, a biomarker for duodenal ulcers and stomach cancers)

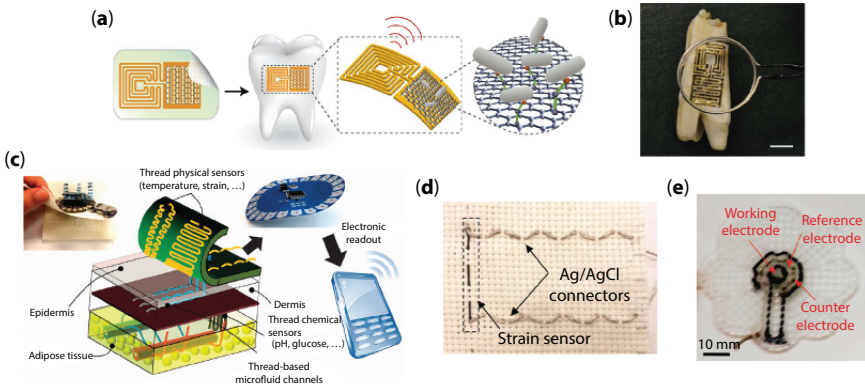

Figure 2.10 Smart nanotextiles for multimodal monitoring of physical and chemical biomarkers. (a) Schematics of tooth-based biosensors composed of functionalized graphene as the sensing element and integrated interdigitated electrode and inductive coil antenna as the wireless readout (reprinted from reference [133], with permission of Springer Nature). (b) Photograph of the tooth-based sensor for remote monitoring of breath and bacteria in saliva. Scale bar, 1 cm (reprinted from reference [133], with permission of Springer Nature). (c) Integrated physical and biochemical sensing platform for wireless health monitoring, where microfluidic channels, sensors, and interconnects are all enabled by threads (reprinted from reference [134], no permission is necessary under the terms of Creative Commons CC BY license). (d) Photograph of the embroidered thread-based strain sensor and interconnects (reprinted from reference [134], no permission is necessary under the terms of Creative Commons CC BY license). (e) Photograph of the embroidered thread-based glucose sensor (reprinted from reference [134], no permission is necessary under the terms of Creative Commons CC BY license).

in saliva alters the resistance of the graphene sensor and accordingly changes the resonance frequency and bandwidth detected from a reader coil antenna (Figure 2.10b). The combination of wearable biosensor and wireless transmission modules facilitates battery-free and remote monitoring. Compared with the widely used Bluetooth for wireless communications, this passive wireless module is simple in architecture and eliminates the need for an on-board power source [15].

Another noteworthy platform that integrates both physical and biochemical sensors is highlighted in Figure 2.10c, where microfluidic channels, sensors, and interconnects are all enabled by threads [134]. To create microfluidic channels for the collection and delivery of fluid analytes, hydrophilic threads were embroidered onto a hydrophobic woven fabric. Conductive threads infused with diverse functional materials (i.e. CNTs, carbon nanopowders, polyaniline, and Ag/AgCl) are employed as sensing elements for strain, temperature, pH, and glucose sensors (Figures 2.10d and 2.10e). Flexible conductive threads are used for interconnections with electronics for data acquisition, processing, and wireless communication. *In vivo* experiments on rats were performed to demonstrate the capabilities of quantifying gastric and subcutaneous pH, as well as the strain associated with different would closure status.

2.5 Conclusions and Future Remarks

As an integral part of the body, smart nanotextiles offer an unobtrusive way to collect paramount physiological parameters and have progressively changed the landscape of healthcare [92, 94, 135]. By facilitating early diagnosis, therapeutic prevention, and informative disease management, smart nanotextiles provide a viable solution to reducing healthcare expenses. These benefits have driven up the market size. According to a report conducted by Grand View Research, the global revenue for medical textiles was $16.7 billion in 2018 and expected to reach $23.3 billion by 2025, increasing at a compound annual growth rate (CAGR) of 4.9% for the period of 2018 to 2025 [136]. The global market for nanotextiles is projected to grow at a CAGR of 23.6% and anticipated to reach $14.8 billion by 2024 from $5.1 billion in 2019. Increasing demands for wearable medical devices is one of the major factors that drive the nanotextile market across the globe [137].

Despite the inspiring progress, the research on nanotextiles remains at the stage of proof-of-concept demonstrations in lab settings, far from being satisfactory for consumer-level devices. Several challenges need to

be addressed before we can take full advantage of health monitoring based on nanotextiles. One grand challenge arises from the rough, curve, and porous surfaces of textiles as compared to planar substrates, which poses a challenge to the scalable fabrication process [14, 138–140]. For example, surface treatment of textiles is often required to modify the water contact angle and roughness for improved printing quality [45, 103, 105]. With respect to continuous wearable applications, the long-term biocompatibility over extended daily wear, as well as the structural and functional integrity under repeated deformations and complex biological environments need to be systematically studied. Furthermore, innovations on biocompatible encapsulation techniques that can improve the resistance to humidity, sweat, oxygen, and washing process are highly desirable. The development of nanotextile also necessitates continued efforts on scale-up manufacturing techniques and optimal human factor designs to ensure wide user adoption.

Acknowledgments

S.Y. would like to acknowledge the support from the start-up fund of the Department of Mechanical Engineering at Stony Brook University and the SBU-BNL seed grant 1168726-9-63845. In addition, the authors gratefully acknowledge the financial support from the National Science Foundation (NSF) through award Nos. 2129673, 2122841, 2134664, and the National Institutes of Health (NIH) under award 1R01HD108473.

References

1. Takei, K., Honda, W., Harada, S., Arie, T., Akita, S., Toward flexible and wearable human-interactive health-monitoring devices. *Adv. Healthc. Mater.*, 4, 487–500, 2015.
2. Trung, T.Q. and Lee, N.E., Flexible and stretchable physical sensor integrated platforms for wearable human-activity monitoring and personal healthcare. *Adv. Mater.*, 28, 4338–4372, 2016.
3. Yetisen, A.K., Martinez-Hurtado, J.L., Ünal, B., Khademhosseini, A., Butt, H., Wearables in medicine. *Adv. Mater.*, 30, 1706910, 2018.
4. Wu, W. and Haick, H., Materials and wearable devices for autonomous monitoring of physiological markers. *Adv. Mater.*, 30, 1705024, 2018.
5. Di, J., Yao, S., Ye, Y., Cui, Z., Yu, J., Ghosh, T.K., Zhu, Y., Gu, Z., Stretch-triggered drug delivery from wearable elastomer films containing therapeutic depots. *ACS Nano*, 9, 9407–9415, 2015.

6. Yao, S., Swetha, P., Zhu, Y., Nanomaterial-enabled wearable sensors for healthcare. *Adv. Healthc. Mater.*, 7, 1700889, 2018.
7. Yao, S. and Zhu, Y., Nanomaterial-enabled dry electrodes for electrophysiological sensing: A review. *JOM*, 68, 1145–1155, 2016.
8. Choi, C., Lee, Y., Cho, K.W., Koo, J.H., Kim, D.-H., Wearable and implantable soft bioelectronics using two-dimensional materials. *Acc. Chem. Res.*, 52, 73–81, 2018.
9. Shi, J., Liu, S., Zhang, L., Yang, B., Shu, L., Yang, Y., Ren, M., Wang, Y., Chen, J., Chen, W., Chai, Y., Tao, X., Smart textile-integrated microelectronic systems for wearable applications. *Adv. Mater.*, 32, 1901958, 2020.
10. Castano, L.M. and Flatau, A.B., Smart fabric sensors and e-textile technologies: A review. *Smart Mater. Struct.*, 23, 053001, 2014.
11. Liu, Y., Pharr, M., Salvatore, G.A., Lab-on-skin: A review of flexible and stretchable electronics for wearable health monitoring. *ACS Nano*, 11, 9614–9635, 2017.
12. Lee, J., Zambrano, B.L., Woo, J., Yoon, K., Lee, T., Recent advances in 1d stretchable electrodes and devices for textile and wearable electronics: Materials, fabrications, and applications. *Adv. Mater.*, 32, 1902532, 2020.
13. Zeng, W., Shu, L., Li, Q., Chen, S., Wang, F., Tao, X.M., Fiber-based wearable electronics: A review of materials, fabrication, devices, and applications. *Adv. Mater.*, 26, 5310–5336, 2014.
14. Wang, L., Fu, X., He, J., Shi, X., Chen, T., Chen, P., Wang, B., Peng, H., Application challenges in fiber and textile electronics. *Adv. Mater.*, 32, 1901971, 2020.
15. Yao, S., Ren, P., Song, R., Liu, Y., Huang, Q., Dong, J., O'Connor, B.T., Zhu, Y., Nanomaterial-enabled flexible and stretchable sensing systems: Processing, integration, and applications. *Adv. Mater.*, 32, 1902343, 2020.
16. Heo, J.S., Eom, J., Kim, Y.H., Park, S.K., Recent progress of textile-based wearable electronics: A comprehensive review of materials, devices, and applications. *Small*, 14, 1703034, 2018.
17. Yao, S. and Zhu, Y., Nanomaterial-enabled stretchable conductors: Strategies, materials and devices. *Adv. Mater.*, 27, 1480–1511, 2015.
18. Khan, Y., Ostfeld, A.E., Lochner, C.M., Pierre, A., Arias, A.C., Monitoring of vital signs with flexible and wearable medical devices. *Adv. Mater.*, 28, 4373–4395, 2016.
19. Liu, Y., Wang, H., Zhao, W., Zhang, M., Qin, H., Xie, Y., Flexible, stretchable sensors for wearable health monitoring: Sensing mechanisms, materials, fabrication strategies and features. *Sensors*, 18, 645, 2018.
20. Gao, Y., Yu, L., Yeo, J.C., Lim, C.T., Flexible hybrid sensors for health monitoring: Materials and mechanisms to render wearability. *Adv. Mater.*, 32, 1902133, 2020.
21. Ray, T.R., Choi, J., Bandodkar, A.J., Krishnan, S., Gutruf, P., Tian, L., Ghaffari, R., Rogers, J.A., Bio-integrated wearable systems: A comprehensive review. *Chem. Rev.*, 119, 5461–5533, 2019.

22. Ha, M., Lim, S., Ko, H., Wearable and flexible sensors for user-interactive health-monitoring devices. *J. Mater. Chem. B*, 6, 4043–4064, 2018.
23. Li, Q., Zhang, L.N., Tao, X.M., Ding, X., Review of flexible temperature sensing networks for wearable physiological monitoring. *Adv. Healthc. Mater.*, 6, 1601371, 2017.
24. Servati, A., Zou, L., Wang, Z.J., Ko, F., Servati, P., Novel flexible wearable sensor materials and signal processing for vital sign and human activity monitoring. *Sensors*, 17, 1622, 2017.
25. Guo, J., Zhou, B., Yang, C., Dai, Q., Kong, L., Stretchable and temperature-sensitive polymer optical fibers for wearable health monitoring. *Adv. Funct. Mater.*, 29, 1902898, 2019.
26. Blasdel, N.J., Wujcik, E.K., Carletta, J.E., Lee, K.-S., Monty, C.N., Fabric nanocomposite resistance temperature detector. *IEEE Sens. J.*, 15, 300–306, 2014.
27. Hua, C., Shang, Y., Li, X., Hu, X., Wang, Y., Wang, X., Zhang, Y., Li, X., Duan, H., Cao, A., Helical graphene oxide fibers as a stretchable sensor and an electrocapillary sucker. *Nanoscale*, 8, 10659–10668, 2016.
28. Zhao, J., Zhang, Y., Huang, Y., Xie, J., Zhao, X., Li, C., Qu, J., Zhang, Q., Sun, J., He, B., Li, Q., Lu, C., Xu, X., Lu, W., Li, L., Yao, Y., 3d printing fiber electrodes for an all-fiber integrated electronic device via hybridization of an asymmetric supercapacitor and a temperature sensor. *Adv. Sci.*, 5, 1801114, 2018.
29. Sibinski, M., Jakubowska, M., Sloma, M., Flexible temperature sensors on fibers. *Sensors*, 10, 7934–7946, 2010.
30. Liao, X., Liao, Q., Zhang, Z., Yan, X., Liang, Q., Wang, Q., Li, M., Zhang, Y., A highly stretchable zno@ fiber-based multifunctional nanosensor for strain/temperature/uv detection. *Adv. Funct. Mater.*, 26, 3074–3081, 2016.
31. Gong, M., Wan, P., Ma, D., Zhong, M., Liao, M., Ye, J., Shi, R., Zhang, L., Flexible breathable nanomesh electronic devices for on-demand therapy. *Adv. Funct. Mater.*, 29, 1902127, 2019.
32. Hong, S.Y., Lee, Y.H., Park, H., Jin, S.W., Jeong, Y.R., Yun, J., You, I., Zi, G., Ha, J.S., Stretchable active matrix temperature sensor array of polyaniline nanofibers for electronic skin. *Adv. Mater.*, 28, 930–935, 2016.
33. Li, Q., Chen, H., Ran, Z.-Y., Zhang, L.-N., Xiang, R.-F., Wang, X., Tao, X.-M., Ding, X., Full fabric sensing network with large deformation for continuous detection of skin temperature. *Smart Mater. Struct.*, 27, 105017, 2018.
34. Shang, Y., Li, Y., He, X., Du, S., Zhang, L., Shi, E., Wu, S., Li, Z., Li, P., Wei, J., Wang, K., Zhu, H., Wu, D., Cao, A., Highly twisted double-helix carbon nanotube yarns. *ACS Nano*, 7, 1446–1453, 2013.
35. Rosace, G., Trovato, V., Colleoni, C., Caldara, M., Re, V., Brucale, M., Piperopoulos, E., Mastronardo, E., Milone, C., De Luca, G., Plutino, M.R., Structural and morphological characterizations of mwcnts hybrid coating onto cotton fabric as potential humidity and temperature wearable sensor. *Sens. Actuators B Chem.*, 252, 428–439, 2017.

36. Cui, Z., Poblete, F.R., Zhu, Y., Tailoring the temperature coefficient of resistance of silver nanowire nanocomposites and their application as stretchable temperature sensors. *ACS Appl. Mater. Interfaces*, 11, 17836–17842, 2019.
37. Wang, C., Hwang, D., Yu, Z., Takei, K., Park, J., Chen, T., Ma, B., and Javey, A., User-interactive electronic skin for instantaneous pressure visualization. *Nat. Mater.*, 12, 899–904, 2013.
38. Cheng, J., Zhou, B., Lukowicz, P., Seoane, F., Varga, M., Mehmann, A., Chabrecek, P., Gaschler, W., Goenner, K., Horter, H., Schneegass, S., Hassib, M., Schmidt, A., Freund, M., Zhang, R., Amft, O., Textile building blocks: Toward simple, modularized, and standardized smart textile, in: *Smart textiles*, pp. 303–331, Springer, Cham, Switzerland, 2017.
39. Coskey, R.J., Contact dermatitis caused by ecg electrode jelly. *Arch. Dermatol.*, 113, 839–840, 1977.
40. Uter, W. and Schwanitz, H., Contact dermatitis from propylene glycol in ecg electrode gel. *Contact Derm.*, 34, 230–231, 1996.
41. Ho, D.H., Cheon, S., Hong, P., Park, J.H., Suk, J.W., Kim, D.H., Han, J.T., Cho, J.H., Multifunctional smart textronics with blow-spun nonwoven fabrics. *Adv. Funct. Mater.*, 29, 1900025, 2019.
42. Lam, C.L., Rajdi, N.N.Z.M., Wicaksono, D.H., Mwcnt/cotton-based flexible electrode for electrocardiography. *IEEE Sensors*, Baltimore, USA, IEEE, 2013.
43. Kumar, P.S., Rai, P., Oh, S., Kwon, H., Varadan, V.K., *Nanocomposite electrodes for smartphone enabled healthcare garments: E-bra and smart vest*, Nanosystems in Engineering, and Medicine, Incheon, Korea, International Society for Optics and Photonics, 2012.
44. Yapici, M.K., Alkhidir, T., Samad, Y.A., Liao, K., Graphene-clad textile electrodes for electrocardiogram monitoring. *Sens. Actuators B Chem.*, 221, 1469–1474, 2015.
45. Karim, N., Afroj, S., Malandraki, A., Butterworth, S., Beach, C., Rigout, M., Novoselov, K.S., Casson, A.J., Yeates, S.G., All inkjet-printed graphene-based conductive patterns for wearable e-textile applications. *J. Mater. Chem. C*, 5, 11640–11648, 2017.
46. Yao, S., Yang, J., Poblete, F.R., Hu, X., Zhu, Y., Multifunctional electronic textiles using silver nanowire composites. *ACS Appl. Mater. Interfaces*, 11, 31028–31037, 2019.
47. Myers, A.C., Huang, H., Zhu, Y., Wearable silver nanowire dry electrodes for electrophysiological sensing. *RSC Adv.*, 5, 11627–11632, 2015.
48. Qin, Q., Li, J., Yao, S., Liu, C., Huang, H., Zhu, Y., Electrocardiogram of a silver nanowire based dry electrode: Quantitative comparison with the standard ag/agcl gel electrode. *IEEE Access*, 7, 20789–20800, 2019.
49. Jin, H., Nayeem, M.O.G., Lee, S., Matsuhisa, N., Inoue, D., Yokota, T., Hashizume, D., Someya, T., Highly durable nanofiber-reinforced elastic conductors for skin-tight electronic textiles. *ACS Nano*, 13, 7905–7912, 2019.

50. Wei, S., Yin, R., Tang, T., Wu, Y., Liu, Y., Wang, P., Wang, K., Mei, M., Zou, R., Duan, X., Gas-permeable, irritation-free, transparent hydrogel contact lens devices with metal-coated nanofiber mesh for eye interfacing. *ACS Nano*, 13, 7920–7929, 2019.
51. Oh, T., II, Yoon, S., Kim, T.E., Wi, H., Kim, K.J., Woo, E.J., Sadleir, R.J., Nanofiber web textile dry electrodes for long-term biopotential recording. *IEEE Trans. Biomed.*, 7, 204–211, 2012.
52. Miyamoto, A., Lee, S., Cooray, N.F., Lee, S., Mori, M., Matsuhisa, N., Jin, H., Yoda, L., Yokota, T., Itoh, A., Sekino, M., Kawasaki, H., Ebihara, T., Amagai, M., and Someya, T., Inflammation-free, gas-permeable, lightweight, stretchable on-skin electronics with nanomeshes. *Nat. Nanotechnol.*, 12, 907–913, 2017.
53. Zhou, W., Yao, S., Wang, H., Du, Q., Ma, Y., Zhu, Y., Gas-permeable, ultrathin, stretchable epidermal electronics with porous electrodes. *ACS Nano*, 14, 5798–5805, 2020.
54. Qureshi, A., II and Caplan, L.R., Intracranial atherosclerosis. *Lancet*, 383, 984–998, 2014.
55. Yusuf, S., Wood, D., Ralston, J., Reddy, K.S., The world heart federation's vision for worldwide cardiovascular disease prevention. *Lancet*, 386, 399–402, 2015.
56. Meng, K., Chen, J., Li, X., Wu, Y., Fan, W., Zhou, Z., He, Q., Wang, X., Fan, X., Zhang, Y., Yang, J., Wang, Z.L., Flexible weaving constructed self-powered pressure sensor enabling continuous diagnosis of cardiovascular disease and measurement of cuffless blood pressure. *Adv. Funct. Mater.*, 29, 1806388, 2019.
57. Wichman, K., Rydén, G., Wichman, M., The influence of different positions and korotkoff sounds on the blood pressure measurements in pregnancy. *Acta Obstet. Gynecol. Scand.*, 63, 25–28, 1984.
58. Costello, B.T., Schultz, M.G., Black, J.A., Sharman, J.E., Evaluation of a brachial cuff and suprasystolic waveform algorithm method to noninvasively derive central blood pressure. *Am. J. Hypertens.*, 28, 480–486, 2015.
59. Elgendi, M., On the analysis of fingertip photoplethysmogram signals. *Curr. Cardiol. Rev.*, 8, 14–25, 2012.
60. Liu, Y., Tao, L.-Q., Wang, D.-Y., Zhang, T.-Y., Yang, Y., Ren, T.-L., Flexible, highly sensitive pressure sensor with a wide range based on graphene-silk network structure. *Appl. Phys. Lett.*, 110, 123508, 2017.
61. Ge, J., Sun, L., Zhang, F.R., Zhang, Y., Shi, L.A., Zhao, H.Y., Zhu, H.W., Jiang, H.L., Yu, S.H., A stretchable electronic fabric artificial skin with pressure-, lateral strain-, and flexion-sensitive properties. *Adv. Mater.*, 28, 722–728, 2016.
62. Wang, C., Li, X., Gao, E., Jian, M., Xia, K., Wang, Q., Xu, Z., Ren, T., Zhang, Y., Carbonized silk fabric for ultrastretchable, highly sensitive, and wearable strain sensors. *Adv. Mater.*, 28, 6640–6648, 2016.

63. Liu, M., Pu, X., Jiang, C., Liu, T., Huang, X., Chen, L., Du, C., Sun, J., Hu, W., Wang, Z.L., Large-area all-textile pressure sensors for monitoring human motion and physiological signals. *Adv. Mater.*, 29, 1703700, 2017.
64. Nan, N., He, J., You, X., Sun, X., Zhou, Y., Qi, K., Shao, W., Liu, F., Chu, Y., Ding, B., A stretchable, highly sensitive, and multimodal mechanical fabric sensor based on electrospun conductive nanofiber yarn for wearable electronics. *Adv. Mater. Technol.*, 4, 1800338, 2019.
65. Li, T., Chen, L., Yang, X., Chen, X., Zhang, Z., Zhao, T., Li, X., Zhang, J., A flexible pressure sensor based on an mxene–textile network structure. *J. Mater. Chem. C*, 7, 1022–1027, 2019.
66. Zhou, Y., He, J., Wang, H., Qi, K., Nan, N., You, X., Shao, W., Wang, L., Ding, B., Cui, S., Highly sensitive, self-powered and wearable electronic skin based on pressure-sensitive nanofiber woven fabric sensor. *Sci. Rep.*, 7, 1–9, 2017.
67. Pang, C., Lee, G.-Y., Kim, T.-I., Kim, S.M., Kim, H.N., Ahn, S.-H., Suh, K.-Y., A flexible and highly sensitive strain-gauge sensor using reversible interlocking of nanofibres. *Nat. Mater.*, 11, 795–801, 2012.
68. Park, S.-H., Lee, H.B., Yeon, S.M., Park, J., Lee, N.K., Flexible and stretchable piezoelectric sensor with thickness-tunable configuration of electrospun nanofiber mat and elastomeric substrates. *ACS Appl. Mater. Interfaces*, 8, 24773–24781, 2016.
69. Lin, M.-F., Xiong, J., Wang, J., Parida, K., Lee, P.S., Core-shell nanofiber mats for tactile pressure sensor and nanogenerator applications. *Nano Energy*, 44, 248–255, 2018.
70. Lawes, C.M., Vander Hoorn, S., Rodgers, A., Global burden of blood-pressure-related disease, 2001. *Lancet*, 371, 1513–1518, 2008.
71. Okamoto, R., Kumagai, E., Kai, H., Shibata, R., Ohtsubo, T., Kawano, H., Fujiwara, A., Ito, M., Fukumoto, Y., Arima, H., Effects of lowering diastolic blood pressure to < 80 mmhg on cardiovascular mortality and events in patients with coronary artery disease: A systematic review and meta-analysis. *Hypertens. Res.*, 42, 650–659, 2019.
72. Kai, H., Kimura, T., Fukuda, K., Fukumoto, Y., Kakuma, T., Furukawa, Y., Impact of low diastolic blood pressure on risk of cardiovascular death in elderly patients with coronary artery disease after revascularization. *Circ. J.*, 80, 1232–1241, 2016.
73. McEvoy, J.W., Chen, Y., Rawlings, A., Hoogeveen, R.C., Ballantyne, C.M., Blumenthal, R.S., Coresh, J., Selvin, E., Diastolic blood pressure, subclinical myocardial damage, and cardiac events: Implications for blood pressure control. *J. Am. Coll. Cardiol.*, 68, 1713–1722, 2016.
74. Lee, S., Reuveny, A., Reeder, J., Lee, S., Jin, H., Liu, Q., Yokota, T., Sekitani, T., Isoyama, T., Abe, Y., Suo, Z., Someya, T., A transparent bending-insensitive pressure sensor. *Nat. Nanotechnol.*, 11, 472, 2016.
75. Kweon, O.Y., Lee, S.J., Oh, J.H., Wearable high-performance pressure sensors based on three-dimensional electrospun conductive nanofibers. *NPG Asia Mater.*, 10, 540–551, 2018.

76. Peter, L., Noury, N., Cerny, M., A review of methods for non-invasive and continuous blood pressure monitoring: Pulse transit time method is promising?. *IRBM*, 35, 271–282, 2014.
77. Ma, Y., Choi, J., Hourlier-Fargette, A., Xue, Y., Chung, H.U., Lee, J.Y., Wang, X., Xie, Z., Kang, D., Wang, H., Han, S., Kang, S.-K., Kang, Y., Yu, X., Slepian, M.J., Raj, M.S., Model, J.B., Feng, X., Ghaffari, R., Rogers, J.A., Huang, Y., Relation between blood pressure and pulse wave velocity for human arteries. *Proc. Natl. Acad. Sci. U. S. A.*, 115, 11144–11149, 2018.
78. Luo, N., Dai, W., Li, C., Zhou, Z., Lu, L., Poon, C.C., Chen, S.C., Zhang, Y., Zhao, N., Flexible piezoresistive sensor patch enabling ultralow power cuffless blood pressure measurement. *Adv. Funct. Mater.*, 26, 1178–1187, 2016.
79. Kim, J. and Kim, W.S., A paired stretchable printed sensor system for ambulatory blood pressure monitoring. *Sens. Actuator A Phys.*, 238, 329–336, 2016.
80. Atalay, O., Kennon, W.R., Demirok, E., Weft-knitted strain sensor for monitoring respiratory rate and its electro-mechanical modeling. *IEEE Sens. J.*, 15, 110–122, 2014.
81. Folke, M., Cernerud, L., Ekström, M., Hök, B., Critical review of noninvasive respiratory monitoring in medical care. *Med. Biol. Eng. Comput.*, 41, 377–383, 2003.
82. Grenvik, A., Ballou, S., McGinley, E., Millen, J.E., Cooley, W.L., Safar, P., Impedance pneumography: Comparison between chest impedance changes and respiratory volumes in 11 healthy volunteers. *Chest*, 62, 439–443, 1972.
83. Leonard, P., Beattie, T., Addison, P., Watson, J., Standard pulse oximeters can be used to monitor respiratory rate. *Emerg. Med. J.*, 20, 524–525, 2003.
84. Yang, Z., Pang, Y., Han, X.-L., Yang, Y., Ling, J., Jian, M., Zhang, Y., Yang, Y., Ren, T.-L., Graphene textile strain sensor with negative resistance variation for human motion detection. *ACS Nano*, 12, 9134–9141, 2018.
85. Cheng, Y., Wang, R., Sun, J., Gao, L., A stretchable and highly sensitive graphene-based fiber for sensing tensile strain, bending, and torsion. *Adv. Mater.*, 27, 7365–7371, 2015.
86. Cao, Z., Wang, R., He, T., Xu, F., Sun, J., Interface-controlled conductive fibers for wearable strain sensors and stretchable conducting wires. *ACS Appl. Mater. Interfaces*, 10, 14087–14096, 2018.
87. Wang, Y., Wang, L., Yang, T., Li, X., Zang, X., Zhu, M., Wang, K., Wu, D., Zhu, H., Wearable and highly sensitive graphene strain sensors for human motion monitoring. *Adv. Funct. Mater.*, 24, 4666–4670, 2014.
88. Tang, Z., Jia, S., Wang, F., Bian, C., Chen, Y., Wang, Y., Li, B., Highly stretchable core–sheath fibers via wet-spinning for wearable strain sensors. *ACS Appl. Mater. Interfaces*, 10, 6624–6635, 2018.
89. Wang, Q., Jian, M., Wang, C., Zhang, Y., Carbonized silk nanofiber membrane for transparent and sensitive electronic skin. *Adv. Funct. Mater.*, 27, 1605657, 2017.

90. Du, D., Tang, Z., Ouyang, J., Highly washable e-textile prepared by ultrasonic nanosoldering of carbon nanotubes onto polymer fibers. *J. Mater. Chem. C*, 6, 883–889, 2018.
91. Li, B., Xiao, G., Liu, F., Qiao, Y., Li, C.M., Lu, Z., A flexible humidity sensor based on silk fabrics for human respiration monitoring. *J. Mater. Chem. C*, 6, 4549–4554, 2018.
92. Ma, Y., Zhang, Y., Cai, S., Han, Z., Liu, X., Wang, F., Cao, Y., Wang, Z., Li, H., Chen, Y., Feng, X., Flexible hybrid electronics for digital healthcare. *Adv. Mater.*, 32, 1902062, 2020.
93. Ghaffari, R., Choi, J., Raj, M.S., Chen, S., Lee, S.P., Reeder, J.T., Aranyosi, A.J., Leech, A., Li, W., Schon, S., Model, J.B., Rogers, J.A., Soft wearable systems for colorimetric and electrochemical analysis of biofluids. *Adv. Funct. Mater.*, 30, 1907269, 2019.
94. Kim, J., Campbell, A.S., de Ávila, B.E.-F., Wang, J., Wearable biosensors for healthcare monitoring. *Nat. Biotechnol.*, 37, 389–406, 2019.
95. Economou, A., Kokkinos, C., Prodromidis, M., Flexible plastic, paper and textile lab-on-a chip platforms for electrochemical biosensing. *Lab Chip*, 18, 1812–1830, 2018.
96. Bandodkar, A.J., Jeang, W.J., Ghaffari, R., Rogers, J.A., Wearable sensors for biochemical sweat analysis. *Annu. Rev. Anal. Chem.*, 12, 1–22, 2019.
97. Hendrick, E., Frey, M., Herz, E., Wiesner, U., Cellulose acetate fibers with fluorescing nanoparticles for anti-counterfeiting and ph-sensing applications. *J. Eng. Fibers Fabr.*, 5, 21−30, 2010.
98. You, X. and Pak, J.J., Graphene-based field effect transistor enzymatic glucose biosensor using silk protein for enzyme immobilization and device substrate. *Sens. Actuators B Chem.*, 202, 1357–1365, 2014.
99. Lin, Y., Bariya, M., Nyein, H.Y.Y., Kivimäki, L., Uusitalo, S., Jansson, E., Ji, W., Yuan, Z., Happonen, T., Liedert, C., Hiltunen, J., Fan, Z., Javey, A., Porous enzymatic membrane for nanotextured glucose sweat sensors with high stability toward reliable noninvasive health monitoring. *Adv. Funct. Mater.*, 29, 1902521, 2019.
100. Parrilla, M., Ferré, J., Guinovart, T., Andrade, F.J., Wearable potentiometric sensors based on commercial carbon fibres for monitoring sodium in sweat. *Electroanalysis*, 28, 1267–1275, 2016.
101. Jia, W., Bandodkar, A.J., Valdés-Ramírez, G., Windmiller, J.R., Yang, Z., Ramírez, J., Chan, G., Wang, J., Electrochemical tattoo biosensors for real-time noninvasive lactate monitoring in human perspiration. *Anal. Chem.*, 85, 6553–6560, 2013.
102. Wang, L., Wang, L., Zhang, Y., Pan, J., Li, S., Sun, X., Zhang, B., Peng, H., Weaving sensing fibers into electrochemical fabric for real-time health monitoring. *Adv. Funct. Mater.*, 28, 1804456, 2018.
103. Parrilla, M., Cánovas, R., Jeerapan, I., Andrade, F.J., and Wang, J., A textile-based stretchable multi-ion potentiometric sensor. *Adv. Healthc. Mater.*, 5, 996–1001, 2016.

104. Dagdeviren, C., Li, Z., Wang, Z.L., Energy harvesting from the animal/human body for self-powered electronics. *Annu. Rev. Biomed. Eng.*, 19, 85–108, 2017.
105. Jeerapan, I., Sempionatto, J.R., Pavinatto, A., You, J.-M., Wang, J., Stretchable biofuel cells as wearable textile-based self-powered sensors. *J. Mater. Chem. A*, 4, 18342–18353, 2016.
106. Yu, Y., Nyein, H.Y.Y., Gao, W., Javey, A., Flexible electrochemical bioelectronics: The rise of *in situ* bioanalysis. *Adv. Mater.*, 32, 1902083, 2020.
107. Zhao, J., Guo, H., Li, J., Bandodkar, A.J., Rogers, J.A., Body-interfaced chemical sensors for noninvasive monitoring and analysis of biofluids. *Trends Chem.*, 1, 559−571, 2019.
108. Park, J., Kim, J., Kim, S.-Y., Cheong, W.H., Jang, J., Park, Y.-G., Na, K., Kim, Y.-T., Heo, J.H., Lee, C.Y., Lee, J.H., Bien, F., Park, J.-U., Soft, smart contact lenses with integrations of wireless circuits, glucose sensors, and displays. *Sci. Adv.*, 4, eaap9841, 2018.
109. Park, H., Ahn, H., Kim, D.-J., Koo, H., Nanostructured gas sensors integrated into fabric for wearable breath monitoring system. *Proceedings of the 2013 International Symposium on Wearable Computers*, Zurich, Switzerland, Association for Computing Machinery, 2013.
110. Han, J.-W., Kim, B., Li, J., Meyyappan, M., A carbon nanotube based ammonia sensor on cotton textile. *Appl. Phys. Lett.*, 102, 193104, 2013.
111. Du, B., Yang, D., She, X., Yuan, Y., Mao, D., Jiang, Y., Lu, F., Mos2-based all-fiber humidity sensor for monitoring human breath with fast response and recovery. *Sens. Actuators B Chem.*, 251, 180–184, 2017.
112. Liu, L.X., Chen, W., Zhang, H.B., Wang, Q.W., Guan, F., Yu, Z.Z., Flexible and multifunctional silk textiles with biomimetic leaf-like mxene/silver nanowire nanostructures for electromagnetic interference shielding, humidity monitoring, and self-derived hydrophobicity. *Adv. Funct. Mater.*, 29, 1905197, 2019.
113. Choi, S.J., Yu, H., Jang, J.S., Kim, M.H., Kim, S.J., Jeong, H.S., Kim, I.D., Nitrogen-doped single graphene fiber with platinum water dissociation catalyst for wearable humidity sensor. *Small*, 14, 1703934, 2018.
114. Kim, S.-J., Choi, S.-J., Jang, J.-S., Kim, N.-H., Hakim, M., Tuller, H.L., Kim, I.-D., Mesoporous wo3 nanofibers with protein-templated nanoscale catalysts for detection of trace biomarkers in exhaled breath. *ACS Nano*, 10, 5891–5899, 2016.
115. Seesaard, T., Lorwongtragool, P., Kerdcharoen, T., Development of fabric-based chemical gas sensors for use as wearable electronic noses. *Sensors*, 15, 1885–1902, 2015.
116. Wu, X., Han, Y., Zhang, X., Lu, C., Highly sensitive, stretchable, and wash-durable strain sensor based on ultrathin conductive layer@ polyurethane yarn for tiny motion monitoring. *ACS Appl. Mater. Interfaces*, 8, 9936–9945, 2016.

117. Zhang, M., Wang, C., Wang, H., Jian, M., Hao, X., Zhang, Y., Carbonized cotton fabric for high-performance wearable strain sensors. *Adv. Funct. Mater.*, 27, 1604795, 2017.
118. Yan, T., Wang, Z., Pan, Z.-J., A highly sensitive strain sensor based on a carbonized polyacrylonitrile nanofiber woven fabric. *J. Mater. Sci.*, 53, 11917–11931, 2018.
119. Souri, H. and Bhattacharyya, D., Highly sensitive, stretchable and wearable strain sensors using fragmented conductive cotton fabric. *J. Mater. Chem. C*, 6, 10524–10531, 2018.
120. Zhong, W., Liu, C., Xiang, C., Jin, Y., Li, M., Liu, K., Liu, Q., Wang, Y., Sun, G., Wang, D., Continuously producible ultrasensitive wearable strain sensor assembled with three-dimensional interpenetrating ag nanowires/polyolefin elastomer nanofibrous composite yarn. *ACS Appl. Mater. Interfaces*, 9, 42058–42066, 2017.
121. Yao, S. and Zhu, Y., Wearable multifunctional sensors using printed stretchable conductors made of silver nanowires. *Nanoscale*, 6, 2345–2352, 2014.
122. Yao, S., Myers, A., Malhotra, A., Lin, F., Bozkurt, A., Muth, J.F., Zhu, Y., A wearable hydration sensor with conformal nanowire electrodes. *Adv. Healthc. Mater.*, 6, 1601159, 2017.
123. Yao, S., Vargas, L., Hu, X., Zhu, Y., A novel finger kinematic tracking method based on skin-like wearable strain sensors. *IEEE Sens. J.*, 18, 3010–3015, 2018.
124. Yin, B., Wen, Y., Hong, T., Xie, Z., Yuan, G., Ji, Q., Jia, H., Highly stretchable, ultrasensitive, and wearable strain sensors based on facilely prepared reduced graphene oxide woven fabrics in an ethanol flame. *ACS Appl. Mater. Interfaces*, 9, 32054–32064, 2017.
125. Lu, W., Yu, P., Jian, M., Wang, H., Wang, H., Liang, X., Zhang, Y., Molybdenum disulfide nanosheets aligned vertically on carbonized silk fabric as smart textile for wearable pressure-sensing and energy devices. *ACS Appl. Mater. Interfaces*, 12, 11825–11832, 2020.
126. Chen, S., Lou, Z., Chen, D., Jiang, K., Shen, G., Polymer-enhanced highly stretchable conductive fiber strain sensor used for electronic data gloves. *Adv. Mater. Technol.*, 1, 1600136, 2016.
127. Chen, S., Liu, S., Wang, P., Liu, H., Liu, L., Highly stretchable fiber-shaped e-textiles for strain/pressure sensing, full-range human motions detection, health monitoring, and 2d force mapping. *J. Mater. Sci.*, 53, 2995–3005, 2018.
128. Gong, S., Lai, D.T., Su, B., Si, K.J., Ma, Z., Yap, L.W., Guo, P., Cheng, W., Highly stretchy black gold e-skin nanopatches as highly sensitive wearable biomedical sensors. *Adv. Electron. Mater.*, 1, 1400063, 2015.
129. Yang, T., Wang, W., Zhang, H., Li, X., Shi, J., He, Y., Zheng, Q.-S., Li, Z., Zhu, H., Tactile sensing system based on arrays of graphene woven microfabrics: Electromechanical behavior and electronic skin application. *ACS Nano*, 9, 10867–10875, 2015.

130. Gui, Q., He, Y., Gao, N., Tao, X., Wang, Y., A skin-inspired integrated sensor for synchronous monitoring of multiparameter signals. *Adv. Funct. Mater.*, 27, 1702050, 2017.
131. Hu, X., Tian, M., Xu, T., Sun, X., Sun, B., Sun, C., Liu, X., Zhang, X., Qu, L., Multiscale disordered porous fibers for self-sensing and self-cooling integrated smart sportswear. *ACS Nano*, 14, 559–567, 2020.
132. Lin, F., Yao, S., McKnight, M., Zhu, Y., Bozkurt, A., Silver nanowire based wearable sensors for multimodal sensing. *IEEE Topical Conference on Biomedical Wireless Technologies, Networks, and Sensing Systems (BioWireleSS)*, Austin, USA, IEEE, 2016.
133. Mannoor, M.S., Tao, H., Clayton, J.D., Sengupta, A., Kaplan, D.L., Naik, R.R., Verma, N., Omenetto, F.G., McAlpine, M.C., Graphene-based wireless bacteria detection on tooth enamel. *Nat. Commun.*, 3, 763, 2012.
134. Mostafalu, P., Akbari, M., Alberti, K.A., Xu, Q., Khademhosseini, A., Sonkusale, S.R., A toolkit of thread-based microfluidics, sensors, and electronics for 3d tissue embedding for medical diagnostics. *Microsyst. Nanoeng.*, 2, 16039, 2016.
135. Zhang, Y., Ding, J., Qi, B., Tao, W., Wang, J., Zhao, C., Peng, H., Shi, J., Multifunctional fibers to shape future biomedical devices. *Adv. Funct. Mater.*, 29, 1902834, 2019.
136. *Medical textiles market size, share & trends analysis report by fabric (non-woven, knitted, woven), by application and segment forecasts, 2019-2025*, Grand View Research, California, United States, April 2019.
137. *Nanotextiles: Opportunities and global markets*, BCC Research, Massachusetts, United States, May 2019.
138. Huang, Q. and Zhu, Y., Gravure printing of water-based silver nanowire ink on plastic substrate for flexible electronics. *Sci. Rep.*, 8, 1–10, 2018.
139. Cui, Z., Han, Y., Huang, Q., Dong, J., Zhu, Y., Electrohydrodynamic printing of silver nanowires for flexible and stretchable electronics. *Nanoscale*, 10, 6806–6811, 2018.
140. Huang, Q. and Zhu, Y., Printing conductive nanomaterials for flexible and stretchable electronics: A review of materials, processes, and applications. *Adv. Mater. Technol.*, 4, 1800546, 2019.
141. Guo, F., Cui, X., Wang, K., Wei, J., Stretchable and compressible strain sensors based on carbon nanotube meshes. *Nanoscale*, 8, 19352–19358, 2016.
142. Soltanian, S., Servati, A., Rahmanian, R., Ko, F., Servati, P., Highly piezoresistive compliant nanofibrous sensors for tactile and epidermal electronic applications. *J. Mater. Sci.*, 30, 121–129, 2015.
143. Huang, T., He, P., Wang, R., Yang, S., Sun, J., Xie, X., Ding, G., Porous fibers composed of polymer nanoball decorated graphene for wearable and highly sensitive strain sensors. *Adv. Funct. Mater.*, 29, 1903732, 2019.